

AD-A151 379

IN SITU THIN FILM MEASUREMENTS(U) ARIZONA UNIV TUCSON
OPTICAL SCIENCES CENTER E PELLETIER ET AL. 15 DEC 84
EOARD-TR-85-07 AFOSR-84-0024

1/1

UNCLASSIFIED

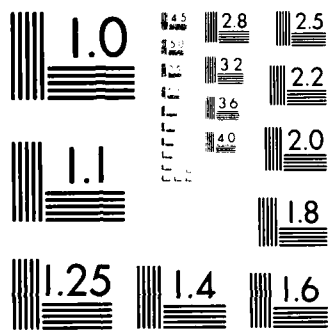
F/G 20/6

NL

END

FILED

DTIC



MICROCOPY RESOLUTION TEST CHART
NATIONAL BUREAU OF STANDARDS-1963-A

Handwritten initials and a circle.

Grant Number AFOSR-84-0024

IN SITU THIN FILM MEASUREMENTS

AD-A151 379

E Pelletier
Ecole Nationale Supérieure de Physique
Domaine Universitaire de Saint Jérôme
13397 MARSEILLE Cedex 13, France

and

H A Macleod
Optical Sciences Center
University of Arizona
Tucson, AZ 85721, USA

15 December, 1984

DTIC
ELECTE
MAR 15 1985
S A D

FINAL REPORT, 15 October, 1983 - 15 October, 1984

Approved for public release;
distribution unlimited

Prepared for
EUROPEAN OFFICE OF AEROSPACE RESEARCH AND DEVELOPMENT
223/231 Old Marylebone Road
London, NW1 5TH, UK

DTIC FILE COPY

IN SITU MEASUREMENT

ABSTRACT

The optical properties of vacuum-deposited thin films were studied in situ during deposition and in air after deposition at the Ecole Nationale Supérieure de Physique, Marseille, and at the Optical Sciences Center, University of Arizona, with the objective of a better understanding of aspects of their behaviour determined largely by their microstructure. The basic measurements that were made in both institutes were similar, T and R after deposition and T during deposition, both as functions of wavelength in the visible and near infrared. The techniques for reducing the measurements to values of n , k and of inhomogeneity differed in certain respects but the results were similar.

Cont'd 1, 3



IN SITU MEASUREMENT

INTRODUCTION

The purposes of this research were twofold. First it was intended to study vacuum-deposited thin films by measurement of their optical properties especially those that would throw light on their microstructure. Second it was hoped that the research could be used as a vehicle to encourage collaboration between the group in Marseille and a similar research group at the Optical Sciences Center in Arizona. This report describes the progress that has been made in both these areas during the year of operation.

The scientific objectives were:

- (a) The measurement of the optical constants of thin-films in air after deposition.
- (b) The measurement of the optical constants of thin films in situ.
- (c) The study of the differences in the measurements under (a) and (b).
- (d) The study of aspects of the thin-film deposition process affecting the film performance as measured under (a) and (b).
- (e) The measurement of optical scattering from thin films and its relation with film structure.

In one year of research it was not expected that all of these topics could receive detailed attention. Nevertheless it was hoped that a solid base for further work and in particular cooperation between the Marseille and Arizona groups could be firmly established. This report described the significant progress that has been made in both of these respects. Of the scientific objectives, (a) and (b) were studied in some detail but only a

IN SITU MEASUREMENT

beginning could be made in respect of (c), (d) and (e).

OPTICAL CONSTANT MEASUREMENT AFTER DEPOSITION

The calculation method is described by Borgogno et al¹. Briefly it consists of the measurement over a wide wavelength range (350-800nm usually) of the parameters T and R, the transmittance and reflectance, respectively, of the thin film on its substrate. These parameters are then used to calculate the refractive index, the extinction coefficient, the thickness and the degree of inhomogeneity of the layer. The model used in this determination exhibits a linear variation of refractive index throughout the layer while the extinction coefficient remains constant. Except for the thickness all of the parameters show dispersion with wavelength.

Work under this heading has been in progress for some considerable time in Marseille. The present contract allowed the completion of a wide survey of optical materials and the study in greater detail of titanium oxide, one of the most important refractory oxides for the visible and near infrared regions. The results are given in Table 1 extracted from Borgogno².

An interesting study involved scandium oxide, a material that may be useful in the near ultraviolet and visible regions but about which little is known. Multiple determinations of the optical constants of scandium oxide thin films that were deposited simultaneously on identical substrates by Optical Coating Laboratory Inc (the Marseille substrates were slightly

IN SITU MEASUREMENT

MATERIAL	A A'	B B'	C C'
ZINC SULPHIDE	2,2524 0	1,5754X10 ⁴ 0	5,4224X10 ⁹ 0
SILICA	1,4625 0	3,0693X10 ³ 0	-2,0190X10 ⁸ 0
ALUMINA	1,6000 -0,02	7,7495X10 ³ 0	-3,9484X10 ³ 0
MAGNESIUM FLUORIDE	1,33619 0	8,1846X10 ³ 0	-5,7723X10 ⁸ 0
ZIRCONIUM OXIDE	2,0125 -0,029	1,4280X10 ⁴ -1,2X10 ⁻⁴	-1,8772X10 ⁷ 0
ZIRCONIUM OXIDE	2,0569 -0,065	-7,1632X10 ³ -1,4X10 ⁻⁴	1,8979X10 ⁷ 1,9X10 ⁻⁷
ZIRCONIUM OXIDE	2,0092 -0,214	-5,3327X10 ³ 8,8X10 ⁻⁴	2,0786X10 ⁹ -8,4X10 ⁻⁷
TANTALUM OXIDE	2,1136 0,018	1,2154X10 ⁴ -8,1X10 ¹	2,2166X10 ⁹ 4,2X10 ⁴

Table 1: Values of A, B(nm²) and C(nm⁴), the Cauchy coefficients in the expansion for refractive index:

$$n = A + B/\lambda^2 + C/\lambda^4$$

and of A', B'(nm₂) and C'(nm⁴), the Cauchy coefficients in the similar expansion for $\Delta n/n_{\text{mean}} = (n_{\text{inner}} - n_{\text{outer}})/n_{\text{mean}}$

IN SITU MEASUREMENT

MATERIAL	A A'	B B'	C C'
TANTALUM OXIDE	2,0841 -0,017	$3,8096 \times 10^3$ $5,2 \times 10^1$	$2,2336 \times 10^9$ $-6,7 \times 10^4$
YTTRIUM OXIDE	1,7493 0	$1,1815 \times 10^4$ 0	$2,0971 \times 10^8$ 0
YTTRIUM OXIDE	1,7525 0,028	$1,7330 \times 10^4$ $-3,4 \times 10^{-5}$	$-2,9163 \times 10^8$ 0
YTTRIUM OXIDE	1,7802 -0,015	$1,2276 \times 10^4$ 0	$-7,0554 \times 10^3$ 0
YTTRIUM OXIDE	1,7969 0,022	$1,1223 \times 10^4$ $-7,7 \times 10^{-5}$	$3,0906 \times 10^7$ 0
YTTRIUM OXIDE	1,8208 0,020	$5,2733 \times 10^3$ 0	$4,9701 \times 10^8$ 0
HAFNIUM OXIDE	1,8998 -0,054	$1,7756 \times 10^4$ $1,9 \times 10^{-5}$	$-5,7327 \times 10^8$ 0
HAFNIUM OXIDE	1,9165 -0,054	$2,1981 \times 10^4$ $1,8 \times 10^{-5}$	$-3,2759 \times 10^8$ 0

Table 1 continued

IN SITU MEASUREMENT

MATERIAL	A	B	C
	A'	B'	C'
HAFNIUM	1,9345	$1,8864 \times 10^4$	$-2,2999 \times 10^8$
OXIDE	-0,040	0	0
TITANIUM	2,0044	$8,7927 \times 10^3$	$5,3890 \times 10^9$
OXIDE	-0,040	0	0
TITANIUM	2,0357	$3,8484 \times 10^4$	$3,7103 \times 10^9$
OXIDE	-0,070	0	0
TITANIUM	2,2658	$-3,4617 \times 10^4$	$11,1686 \times 10^{10}$
OXIDE	-0,040	0	0
TITANIUM	2,3126	$-3,7938 \times 10^4$	$1,2411 \times 10^{10}$
OXIDE	-0,055	0	0
TITANIUM	2,3438	$-1,4159 \times 10^4$	$9,8190 \times 10^9$
OXIDE	-0,048	$-2,69 \times 10^{-4}$	0

Table 1 continued

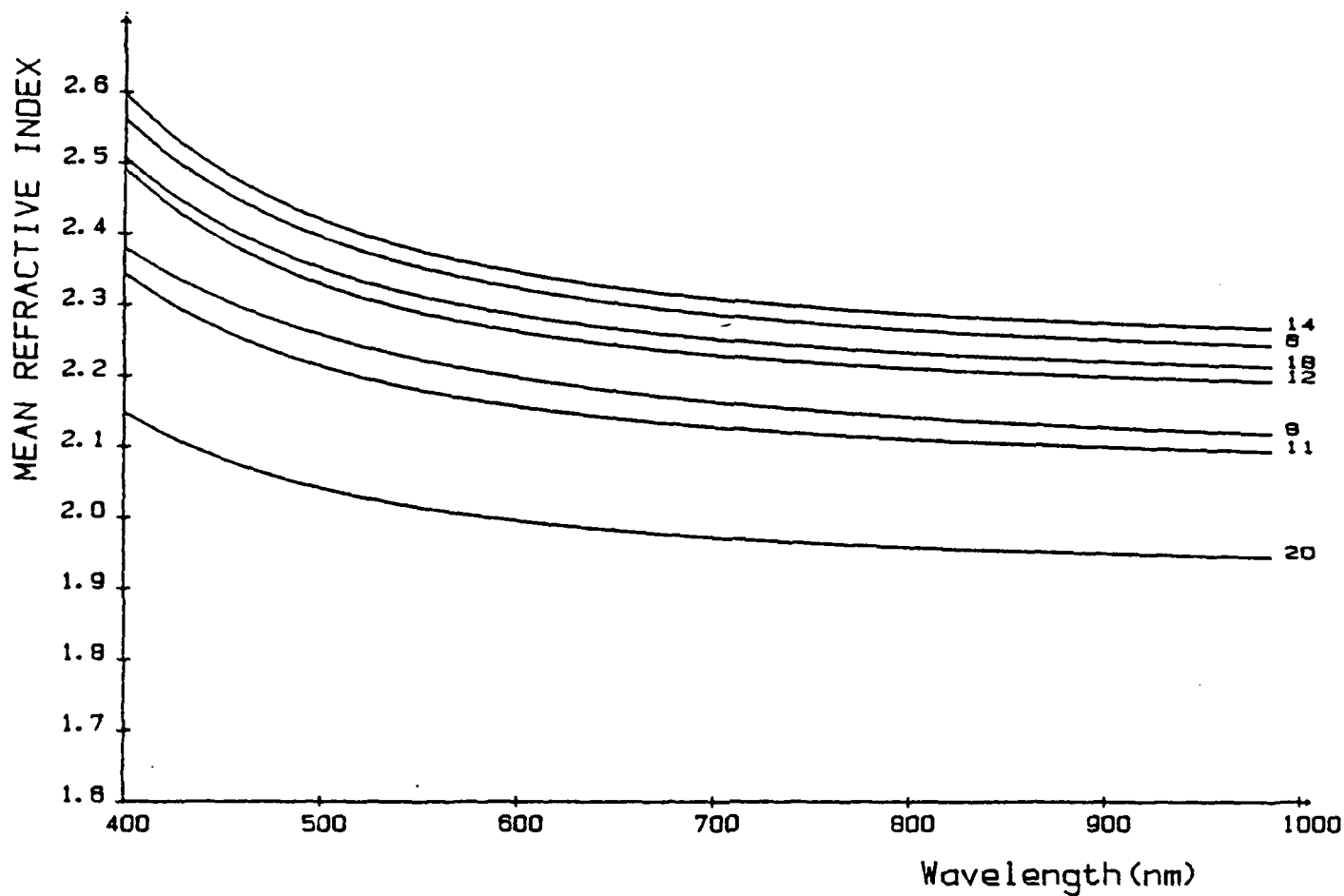
IN SITU MEASUREMENT

wedged and of different shape from the others but of the same material) were arranged to be made by seven different groups including both Marseille and Arizona, who reported their results at the Optical Society of America Fall Meeting in New Orleans at the end of October 1983. A joint paper³ has been published on the investigation. The Marseille group used their normal techniques for reduction of the results: the Arizona group made similar measurements of T and R but used a completely different analytical approach that was developed from a technique⁴ for extracting the optical constants of homogeneous films from measurements of T only. The results of the Marseille and Arizona measurements agreed remarkably well as evidenced by Table 2. The Arizona method uses the envelopes of the transmittance and reflectance characteristics and has been further developed into an in situ measurement technique, to be described later, for inhomogeneous film characterization using T measurements only.

An extensive study of titanium oxide has been made in an attempt to correlate the optical constants with the conditions under which the layers were deposited. This has proved to be an exceedingly complicated topic and no simple theory has so far emerged. The results are extensive and are still not completely analyzed and they are specific to one particular evaporator. A summary of the results has been published by Borgogno et al⁵ and is shown in figure 1. The text of this paper is given as appendix 1.

It is worth emphasising that optical inhomogeneity is found in almost all thin films and this has important implications for the production of high-performance optical coatings especially since the model used in the design and calculation of such multilayers is the common parallel-sided homogeneous slab.

IN SITU MEASUREMENT



TITANIUM OXIDE (measurements in air)

Figure 1. The refractive index of titanium dioxide layers depends strongly on the deposition conditions referred to as a number near each curve. The values of n as a function of wavelength are deduced from reflectance and transmittance measured in air.

IN SITU MEASUREMENT

	WAVELENGTH INNER INDEX		OUTER INDEX		
	nm	ENVELOPE	SPECTROMETRIC	ENVELOPE	SPECTROMETRIC
THIN	333	1,830	1,807	2,038	2,055
FILM	415	1,802	1,814	1,980	1,960
	551	1,775	1,829	1,914	1,908
THICK	315	1,810	1,811	2,021	2,017
FILM	344	1,804	1,804	1,999	2,014
	377	1,796	1,790	2,000	1,995
	421	1,787	1,787	1,993	1,975
	478	1,802	1,790	1,957	1,941
	555	1,810	1,797	1,895	1,909
	668	1,819	1,807	1,847	1,875

Table 2: Comparison of measurements of the refractive indices of scandium oxide made on similar samples after deposition at Optical Sciences (envelope) and Marseille (spectrometric).

IN SITU MEASUREMENTS

In situ measurements are important for several reasons. Accurate control of the process demands an accurate knowledge of the optical constants of the material as it is actually deposited. These are seldom exactly the same as post-deposition values which are frequently perturbed by moisture adsorption. As we have already commented, inhomogeneity of optical constants is the norm rather than exception and there are great difficulties in the estimation of the actual profile of refractive index through the layer from post-deposition results only. Any serious attempt to relate microstructure to optical constants demands a knowledge of the

IN SITU MEASUREMENT

index profile and hence more information than can be obtained from post-deposition measurements.

In situ measurements have been an important objective of the Marseille group for at least ten years and considerable progress has been made in the development of equipment and especially in the signal processing aspects of the problem. Measurements of film transmittance during deposition over a wide spectral range are recorded using a rapid scanning spectrometer. The latest version of the apparatus uses concave holographic diffraction gratings with photodiode arrays of the Reticon type as detectors and the signals are processed by PDP1106 computers. Construction of an in situ monitoring system began in Arizona some three years ago under a DARPA contract through NWC. This system differs from that developed in Marseille in that a CCD detector array is used rather than the Reticon and the computer is an IBM PC⁶. An original intention of the present contract was the provision of the salary of a post-doctoral assistant in the Arizona group who would be chosen from Marseille so that rapid profit could be derived from the Marseille experience. In the event it proved difficult to arrange for this activity to be funded through Marseille and a separate AFOSR contract was placed in the USA to cover it. A separate report covering only this aspect has been submitted to AFOSR. Nevertheless, information is included here for completeness and appendix 2 summarises the design.

In situ measurements have therefore been made both in Marseille and in Arizona. While the measurements were essentially the same, slightly different techniques for the reduction of the measurements to actual index profiles have been used.

IN SITU MEASUREMENT

The method in use in Marseille relies on the fact that the admittance locus for a single homogeneous layer intersects the real axis at the turning values of reflectance. These points of intersection are spaced apart by quarterwave thicknesses. Layers that exhibit only slight inhomogeneity depart to a negligible extent from this condition. The values of the intercepts with the real admittance axis can be readily calculated from the value of reflectance at the turning values. Once these values have been established it is a straightforward matter to calculate the equivalent homogeneous dielectric layer between each and this in turn leads to a curve of index against thickness of the dielectric layer with points every quarterwave. The method is described in greater detail in two publications^{7,8}. One of the materials studied was TiO_2 and some results are reproduced in figure 2. Further measurements were made and reported by Borgogno et al⁵, given as appendix 1. These comprised two sets of measurements and calculations. First the inhomogeneity was measured in the normal way during deposition. These results are shown in figure 3 (figure 6 of appendix 1). Next, after deposition, the same layers were removed from the coating chamber, R and T measurements in air were made, and their optical constants calculated, figure 4 (appendix 1, figure 4). The shift of index between both of these values is shown in figure 5 (appendix 1, figure 7). The differences between the two values of index can largely be attributed to the entry of moisture in the layers but the details of the difference curves indicate that more work is necessary to explain them fully.

The Arizona method is similar to that at Marseille, but relies on a slightly different concept. The method is described in greater detail by

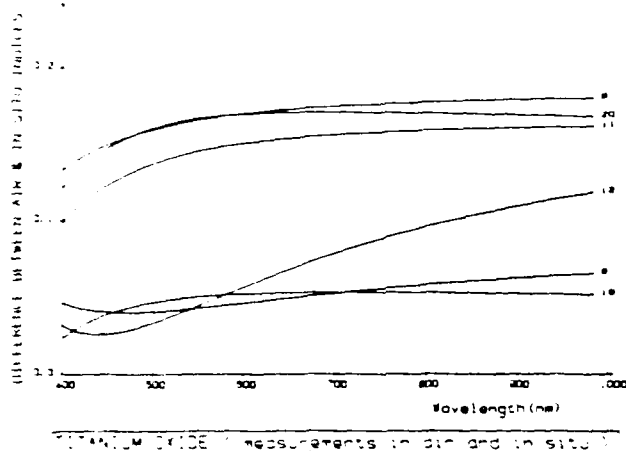


Fig. 7. Differences between the values of the refractive indices measured in air (Fig. 3) and those deduced from *in situ* measurements (Fig. 5).

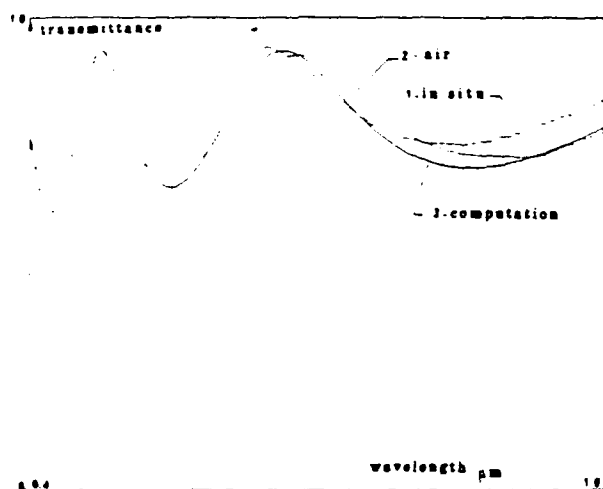


Fig. 8. Measured transmittance of the titanium oxide layer (Ref. 6 of Fig. 3): 1. measured *in situ* at the end of the deposition; 2. measured in air, three days after deposition; 3. calculated after Harris *et al.*⁶

Here, the curve gives the result recorded two days after air admission, the spectral profile being well stabilized.

Figure 9 gives the same measurements made on a sample (Ref. 20, Fig. 3) the mean index of which is much lower. The effect of air admission is considerable.

A first interpretation of these differences is made using the calculation method developed by Harris *et al.*⁶ starting from the values $\bar{n}(\lambda)$ determined *in vacuo*, we calculate the values of the packing coefficient and of the refractive index of the bulk material that explain the properties measured in air. In these calculations, the interstitial medium is water, the index of which $n_2(\lambda)$ is well known. This leads to $p = 0.92$ for the layer of Ref. 6; the corresponding calculated profiles are plotted in Figs. 8 and 9. Agreement with experimental values is far from good.

Knowing that our techniques of index determination that take account of inhomogeneity are proved to be

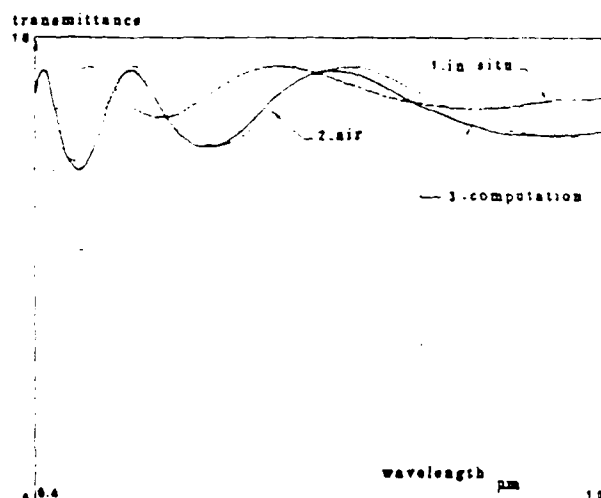


Fig. 9. Measured transmittance of the titanium oxide layer (Ref. 20 of Fig. 3): 1. measured *in situ* at the end of the deposition; 2. measured in air, three days after deposition; 3. calculated after Harris *et al.*⁶

correct for a quasi-perfect explanation of measured optical properties, we hope to be able to introduce this additional parameter and so complete the calculation methods of Macleod for a better interpretation of water adsorption in layers.

The authors wish to thank the DRET which has supported this study. Cooperation between Marseille and Tucson was especially enhanced by an Air Force Office of Scientific Research (AFSOR 84-0024) grant.

This paper was presented at the third topical meeting on Optical Interference Coatings, Monterey, Calif., 17-19 Apr. 1984.

References

1. H. K. Pulker, "Characterization of Optical Thin Films," Appl. Opt. 18, 1969 (1979); H. K. Pulker, G. Paesold, and E. Ritter, "Refractive Indices of TiO_2 Films Produced by Reactive Evaporation of Various Titanium-Oxygen Phases," Appl. Opt. 15, 2956 (1976); E. Ritter, "Dielectric Film Materials for Optical Applications," Phys. Thin Films 8, 1 (1975).
2. H. M. Liddell, *Computer Aided Techniques for the Design of Multilayer Filters* (Adam Hilger, London, 1981); F. Abelès, "Methods for Determining Optical Parameters of Thin Films," Prog. Opt. 2, 250 (1963).
3. J. P. Borgogno, B. Lazarides, and E. Pelletier, "Automatic Determination of the Optical Constants of Inhomogeneous Thin Films," Appl. Opt. 21, 4020 (1982).
4. P. Bousquet and E. Pelletier, "Optical Thin Film Monitoring—Recent Advances and Limitations," Thin Solid Films 77, 165 (1981); H. A. Macleod, "Monitoring of Optical Coatings," Appl. Opt. 20, 82 (1981); E. Pelletier, "Monitoring of Optical Thin Films During Deposition in Thin Film Technologies," Proc. Soc. Photo-Opt. Instrum. Eng. 401, 74 (1983); F. Flory, B. Schmitt, E. Pelletier, and H. A. Macleod, "Interpretation of Wide Band Scans of Growing Optical Thin Films in Terms of Layer Microstructure," Proc. Soc. Photo-Opt. Instrum. Eng. 401, 109 (1983).
5. H. A. Macleod, "Turning Value Monitoring of Narrow-Band All-Dielectric Thin Film Optical Filters," Opt. Acta 19, 1 (1972).
6. M. Harris, H. A. Macleod, S. Ogura, E. Pelletier, and B. Vidal, "The Relationship Between Optical Inhomogeneity and Film Structure," Thin Solid Films 57, 197 (1979).

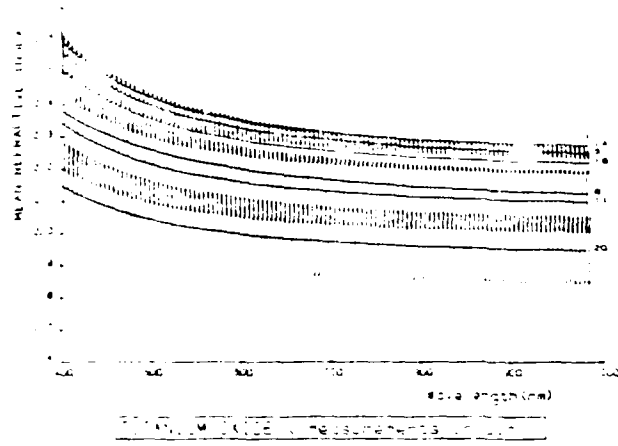


Fig. 4. Inhomogeneity defects of the layers referred to in Fig. 3; $\Delta n = n_{\text{substrate}} - n_{\text{layer}}$ is plotted as a function of wavelength; the index systematically decreases from the substrate.

studied are ~ 320 nm thick, their extinction coefficient k is always smaller than 2×10^{-3} . The evaporated material is the oxide TiO_2 . We cannot give all the details of the different evaporation conditions indicated by a number near each curve. Generally speaking we repeat Pulker's results: the index increases with substrate temperature which varies from 150°C (exp. 20) to 300°C (exp. 6). Many other parameters, such as deposition rate, partial pressure of oxygen, and state of the TiO_2 material in the crucible, can modify the values of \bar{n} .

Concerning homogeneity defects, the problem is even more complicated. Measurements lead to the value $\Delta n/\bar{n}$. We can have either a marked inhomogeneity $\Delta n/\bar{n} \approx -12\%$ (exp. 20) or practically homogeneous layers with $\Delta n/\bar{n} \approx 0$ (exp. 3). The minus sign indicates a decrease of refractive index from the substrate (Fig. 2) ($n_{\text{substrate}} - n_{\text{layer}} = \Delta n$) is systematically negative or null. A general idea of results on the different samples is given in Fig. 4. Around the values of \bar{n} , vertical lines show the amplitude of $n_1 - n_2$. It seems that oxygen partial pressure and preparation (e.g., cleaning) conditions of the substrate (see B₁₄ and silica) have a greater influence on the inhomogeneity ratio than does temperature.

B. In Situ Measurements

The results of *in situ* measurements must be taken with some reservations because we have only transmittance measurements which are less precise than those made in air. But, mainly *in vacuo*, during the growth of the layer, absorption can be disturbing. Sample 14 that gave the higher index in air (see Fig. 3) is not correctly determined, coefficient k being much greater than 5×10^{-3} . For other samples it does not seem that absorption falsifies our measurements.

The mean value of \bar{n} , measured *in vacuo*, is given in Fig. 5. We also have the law of variation of index vs layer thickness for some thirty wavelengths. For an evaporation with a constant deposition rate, the variation law of $n(x)$ is linear. As for Fig. 5 representing measurements in air, we represent the inhomogeneity

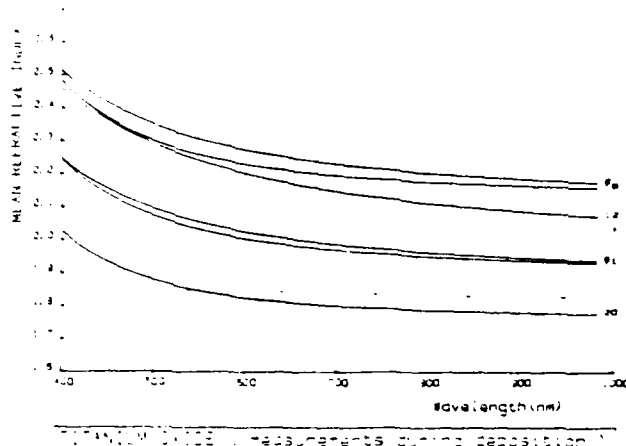


Fig. 5. Refractive index n of titanium dioxide layers of Fig. 3 calculated from *in situ* measurements during deposition.

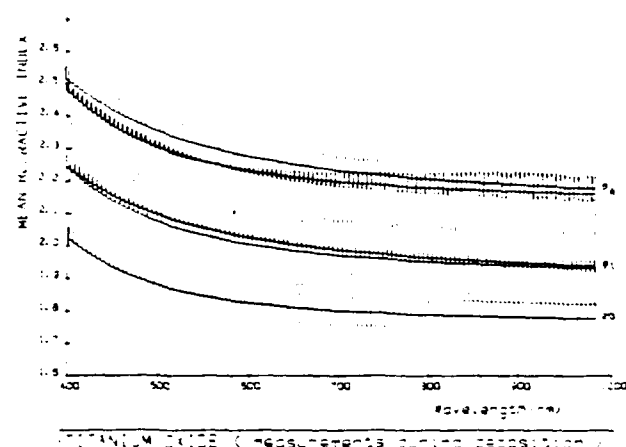


Fig. 6. Inhomogeneity Δn of titanium dioxide layers of Fig. 3 calculated from *in situ* measurements during deposition; the index systematically decreases from the substrate.

detected *in vacuo* by plotting the extreme values ($n_1 - n_2$) of the samples (Fig. 6).

In a general way, inhomogeneity *in vacuo* is greater than that observed in air. We shall see that the variations in the mean index are also significant.

IV. Effect of Air Admission After Deposition

First, let us compare Figs. 3 and 5 to calculate the shift observed in the mean value of the index. Figure 7 gives the differences between indices vs wavelength. This difference varies with sample from 0.05 to 0.15. We can try to separate effects due to the temperature change (between the two measurements) and those due to the phenomenon of water adsorption.

Figure 8 gives transmittance vs wavelength for the sample of Ref. 6, in the 400–1000-nm range. This measurement was made immediately following deposition with a substrate temperature of $\sim 300^\circ\text{C}$. The return to room temperature gives a slight modification of the spectral profile that can just be detected with this spectrometer. But as soon as air is admitted into the chamber, the spectral profile changes spectacularly.

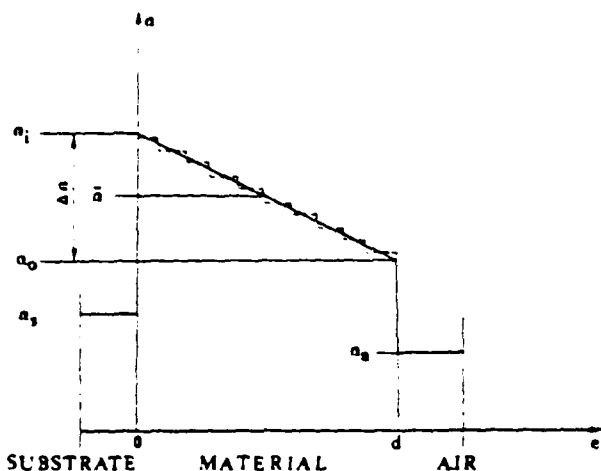


Fig. 1. Model chosen to represent the inhomogeneous layer between media of indices n_s (substrate) and n_a (air). The index of the layer varies from n_i at the inner surface to n_o at the outer. Inhomogeneity is given by $\Delta n/\pi$ which is negative for the index decreasing linearly from substrate to outer surface.

1. In Situ Measurements During Deposition of the Layer

In spite of experimental difficulties which appreciably limit the precision of index determination, knowledge of optical constants of layers in their production conditions is particularly useful,⁴ especially because these values are sometimes different from those measured at normal temperature and pressure.

The principle of the measurement is as follows: The vaporating chamber is equipped with a rapid scanning spectrophotometer which allows us to record the evolution of the transmittance. Figure 2 gives an illustration of the observed phenomenon. Calculations are made systematically for thirty-two wavelengths regularly distributed in the 0.4–1.1- μm range. In these calculations, the extinction coefficient is assumed to be negligible. It is then sufficient to extract, for each wavelength, the extreme values of the transmission detected during the deposition.

Starting from two consecutive values T_i and T_{i+1} , that is, a maximum and a minimum, it is possible to construct the circle of admittance⁵ and to determine the mean value of the refractive index of the thickness deduced when the layer thickness changes from $i\lambda/4$ to $(i+1)\lambda/4$. So, for layers with large optical thicknesses (several $\lambda/4$), we can determine the inhomogeneities, since we have one value for n for each value of the optical thickness z equal to $z = (i + 1/2)\lambda/4$. We shall examine some experimental results derived from these two measurement methods to emphasize the systematically occurring differences and explain their origin.

Inhomogeneity and Index: Dependence on the Deposition Condition

We have systematically studied the optical constants of titanium oxide layers to show how they depend on the deposition conditions. Many studies of this topic,

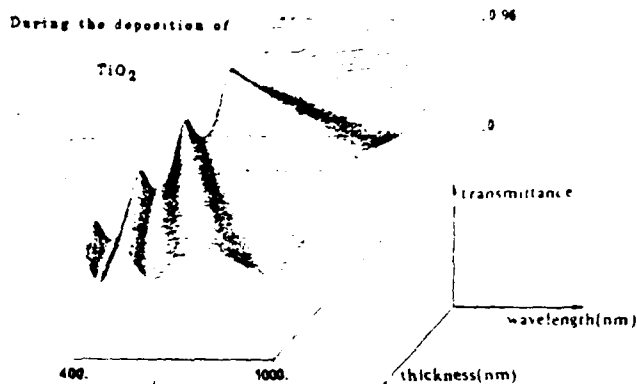


Fig. 2. Three-dimensional plot representing expected development of the transmittance over the 400–1000-nm spectral region during the deposition of a layer of titanium oxide $6\lambda_0/4$ thick with $\lambda_0 = 550$ nm.

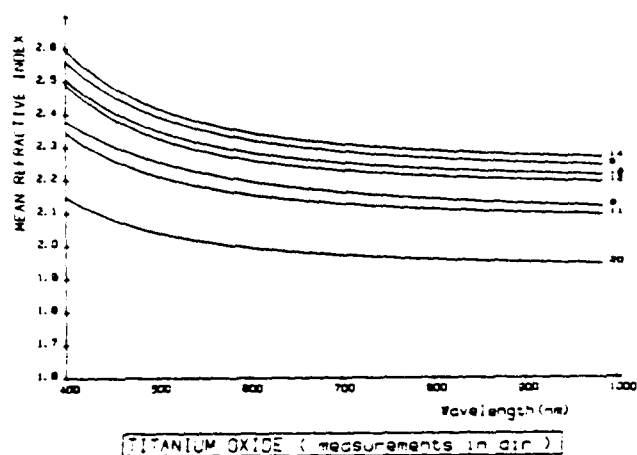


Fig. 3. Refractive index of titanium oxide layers depends strongly on the deposition conditions. The values of \bar{n} as a function of wavelength are deduced from reflectance and transmittance measured in air.

especially by Pulker and Ritter,¹ have been published and they give an idea of the incredible complexity of the behavior of this material evaporated in a reactive atmosphere. The results given here concern refractive indices measured *in vacuo* and these same indices measured after cooling and exposure to atmospheric humidity. They demonstrate the complexity of the problem rather than leading to a better understanding of it.

Nevertheless, we note that knowledge of these values, along with the control of the layer deposition conditions, is absolutely necessary to ensure the accurate manufacture of multilayer stacks. We can give only a general idea of our experimental results.

A. Measurements in Air

Figure 3 shows the dispersion law vs wavelength of the mean value of index \bar{n} , the layers being measured in air.

We have chosen a sample group of layers to show the disparity of the values normally used. All the layers

Refractive index and inhomogeneity of thin films

J. P. Borgogno, F. Flory, P. Roche, B. Schmitt, G. Albrand, E. Pelletier, and H. A. Macleod

The fact that the optical characteristics of thin-film materials are generally different from those of the same materials in bulk form is well known. The differences depend very much on the conditions in which the deposition has been carried out. A good understanding of these differences, their causes, and the influence of deposition parameters is vital if we are to be able to improve coating quality. We have developed two complementary methods with the objective of deriving information on the index of refraction and its variation throughout the thickness of the film. Perceptible optical inhomogeneity is normally present and appreciable inhomogeneity is frequently present in thin films. Such inhomogeneity is usually associated with layer microstructure. The first is a postdeposition technique that makes use of measurements in air of the transmittance and reflectance of the layer under study over a wide wavelength region. The second, in contrast, makes use of *in situ* measurements, that is measurements made under vacuum and during the actual deposition of the layer. We shall show with the help of several examples that the two methods lead to results that are consistent and demonstrate the existence in deposited materials of an inherent variation of the index of refraction normal to the surface. The thermal sensitivity of the layer properties and their tendency to adsorb atmospheric moisture must be taken into account before the residual differences between the two techniques can be explained.

I. Introduction

In the literature¹ are many papers on the influence of evaporation conditions on the stoichiometry and microstructure of evaporated layers. For example, for numerous materials the complex index of refraction obviously depends on these conditions and it is important to take account of this fact in solving the problems of manufacturing optical multielectric filters. In fact, in most cases, the values of refractive indices are deduced from accurate spectrophotometric measurements made on the layers after they are taken out of the evaporating chamber.²

An accurate control of the growth of the layers involves *in situ* knowledge of indices, that is, as they are actually growing. These values can be different from those observed in air, at normal pressure and temperature.

We shall briefly describe the techniques used for determining the indices from the different measure-

ments and, using some examples, we shall show how complicated are the experimental results given by this study.

II. Techniques for Determining Optical Constants

We can distinguish two types of method: measurements made in air and those made *in vacuo* during the deposition of the layers.

A. Measurements in Air³

The principle of the method of determination of optical constants is classical: reflection and transmission factors of a layer, deposited on a prismatic substrate of well-known index, are measured. Our measurements are made over a wide spectral range: from 0.4 and 1.1 μm . In most cases the hypothesis of a homogeneous layer is not sufficient to correctly explain the measured optical properties. For the calculation, the layer is therefore assumed to have a constant index gradient in its thickness and the three following parameters are determined conjointly:

the mean index of complex refraction $n^* = \bar{n} - ik$, which is a function of the wavelength λ ;

the relative variation of index in the thickness of the layer $\Delta n/\bar{n}$ with the sign convention given in Fig. 1;

the geometrical thickness d .

Measurements and calculations are made automatically, and we have done a complete and systematic study in our laboratory to establish the dependence of \bar{n} , k , and $\Delta n/\bar{n}$ on the evaporating conditions of materials generally used in the visible spectral range.

H. A. Macleod is with University of Arizona, Optical Sciences Center, Tucson, Arizona 85721; the other authors are with Ecole Nationale Supérieure de Physique, Centre d'Etude des Couches Minces, U. A. au CNRS, Domaine Universitaire de St. Jérôme, 13397 Marseille CEDEX 13, France.

Received 12 June 1984.

0021-8978/84/201567-04\$02.00.

© 1984 Optical Society of America.

IN SITU MEASUREMENT

APPENDIX 1: J P Borgogno, F Flory, P Roche, B Schmitt, G Albrand, E
Pelletier and H A Macleod
Refractive index and inhomogeneity of thin films
Applied Optics, Vol 23, pp 3567 - 3570, 1984

IN SITU MEASUREMENT

FIGURE CAPTIONS

1. The refractive index of titanium dioxide layers depends strongly on the deposition conditions referred to as a number near each curve. The values of n as a function of wavelength are deduced from reflectance and transmittance measured in air.
2. Titanium oxide. Values of refractive index as a function of thickness. The results are derived from the measurements recorded during the deposition for the wavelengths:
479.0nm ▲ 555.8nm □ 594.2nm ■ 632.6nm o 728.6nm
● 824.6nm
The optical thicknesses $4 \lambda_0/4$ and $8 \lambda_0/4$ are located on the thickness axis. $\lambda_0 = 550 \text{ nm}$
3. The inhomogeneity Δn of titanium dioxide layers of fig. 1 calculated from *in situ* measurements during deposition; the index systematically decreases from the substrate.
4. Homogeneity defects of the layers referred to in figure 1. $\Delta n = n_{\text{inside}} - n_{\text{outside}}$ is plotted as a function of wavelength; the index systematically decreases from the substrate.
5. Difference between the mean values of the refractive indices measured in air and *in situ*.

IN SITU MEASUREMENT

Monitoring of optical thin films during deposition
Proc SPIE, Vol 401, pp 74 - 82, 1983

9. F Flory, B Schmitt, E Pelletier and H A Macleod
Interpretation of wide band scans of growing optical thin films in
terms of layer microstructure
Proc SPIE, Vol 401, pp 109 - 116, 1983

IN SITU MEASUREMENT

REFERENCES

1. J P Borgogno, B Lazarides and E Pelletier
Automatic determination of the optical constants of inhomogeneous thin films
Applied Optics, Vol 21, pp 4020 - 4029, 1982
2. J P Borgogno
Filtres spectraux multidiélectrique: perfectionnement des methodes de synthèse et élaboration d'un modèle de couche rendant compte des propriétés optiques observées
Thèse d'Etat, July, 1984
3. D P Arndt, R M A Azzam, J M Bennett, J P Borgogno, C K Carniglia, W E Case, J A Dobrowolski, U J Gibson, T Tuttle Hart, F C Ho, W P Klapp, H A Macleod, E Pelletier, M K Purvis, D M Quinn, D H Strome, R Swenson, P A Temple and T F Thoun
Multiple determination of the optical constants of thin-film coating materials
Applied Optics, Vol 23, pp 3571 - 3596, 1984
4. J C Manifacier, J Gasiot and J P Fillard
A simple method for the determination of the optical constants n , k and the thickness of a weakly absorbing thin film
J Phys E: Sci Instrum, Vol 9, pp 1002 - 1004, 1976
5. J P Borgogno, F Flory, P Roche, B Schmitt, G Albrand, E Pelletier and H A Macleod
Refractive index and inhomogeneity of thin films
Applied Optics, Vol 23, pp 3567 - 3570, 1984
6. F J Van Milligen, B Bovard, M R Jacobson, J Mueller, R Potoff, R L Shoemaker and H A Macleod
Development of an automatic scanning monochromator for monitoring thin films
Submitted to Applied Optics, 1984
7. B Bovard, F J Van Milligen, M J Messerly, S G Saxe and H A Macleod
Optical constants derivation for an inhomogeneous thin film from in situ transmission measurements
Submitted to Applied Optics, 1984
8. E Pelletier

IN SITU MEASUREMENT

CONCLUSIONS

Techniques for the measurement of thin-film optical constants both during and after deposition have been developed at the Ecole Nationale Supérieure de Physique, Marseille, and the Optical Sciences Center, Arizona. These techniques have been used to study the inhomogeneity of films, especially titanium dioxide, and the way in which the optical constants change with moisture adsorption on exposure to the atmosphere. These aspects of film behaviour are directly related to film microstructure. The collaboration between the two groups has been fruitful, particularly in respect of the contribution that was made to the work at Optical Sciences by B Bovard from Marseille.

IN SITU MEASUREMENT

Bovard et al⁹ which is given as appendix 3. The layer is assumed to have slight inhomogeneity that varies smoothly throughout it. In the case of a lossless dielectric film this leads to a straightforward and slight modification of the normal matrix expression for the film. Small losses can be included by altering the phase thickness to include a complex refractive index. An envelope method⁴ similar to that employed in the post-deposition determination of film indices³ is then used to extract the inner and outer values of refractive index at each stage of film growth. The principal problem is in drawing the envelopes. Numerical techniques for smoothing the curve of transmittance against thickness are first employed and then parabolic expressions are used to generate the envelope curves. Measurements on a typical titanium dioxide layer prepared under good conditions give for a total geometrical thickness of 670nm, an inner refractive index, that is the value next to the substrate, of 2.135 and an outer refractive index of 1.794. The variation of both these parameters with wavelength is given in appendix 3, figure 4.

The method implies the assumption that the layer is sufficiently stable during the measurement that the values of the part already deposited do not change. This can in fact be used as a test for stability. Other measurements of the index profile of a layer prepared under poor oxidising conditions, appendix 3, figure 5, show considerable discontinuities in extinction coefficient that even becomes negative. This indicates a lack of stability of such a layer.

This work represents simply a beginning. We must carry out further comparisons of the two methods. This can even be done on the same data.

IN SITU MEASUREMENT

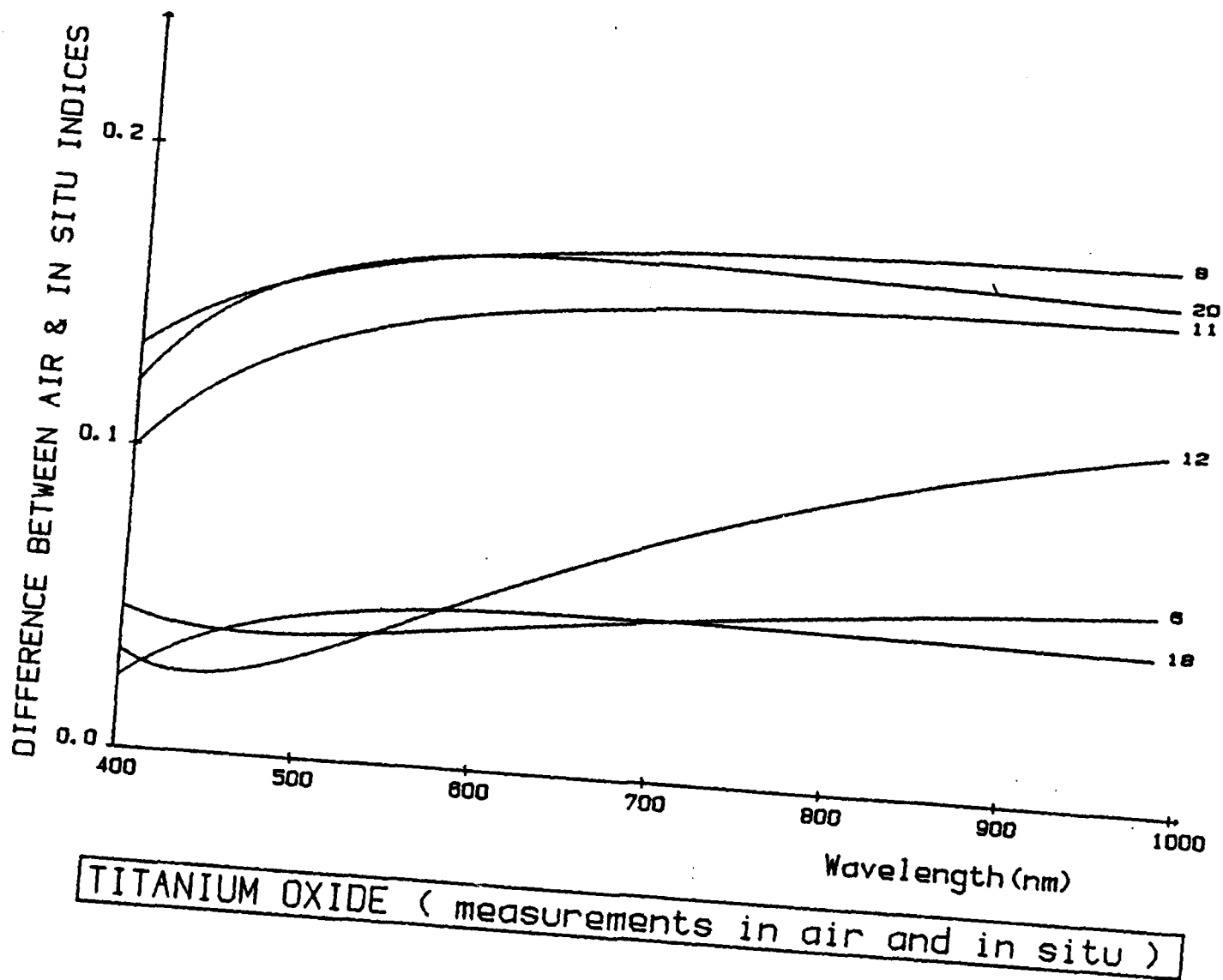
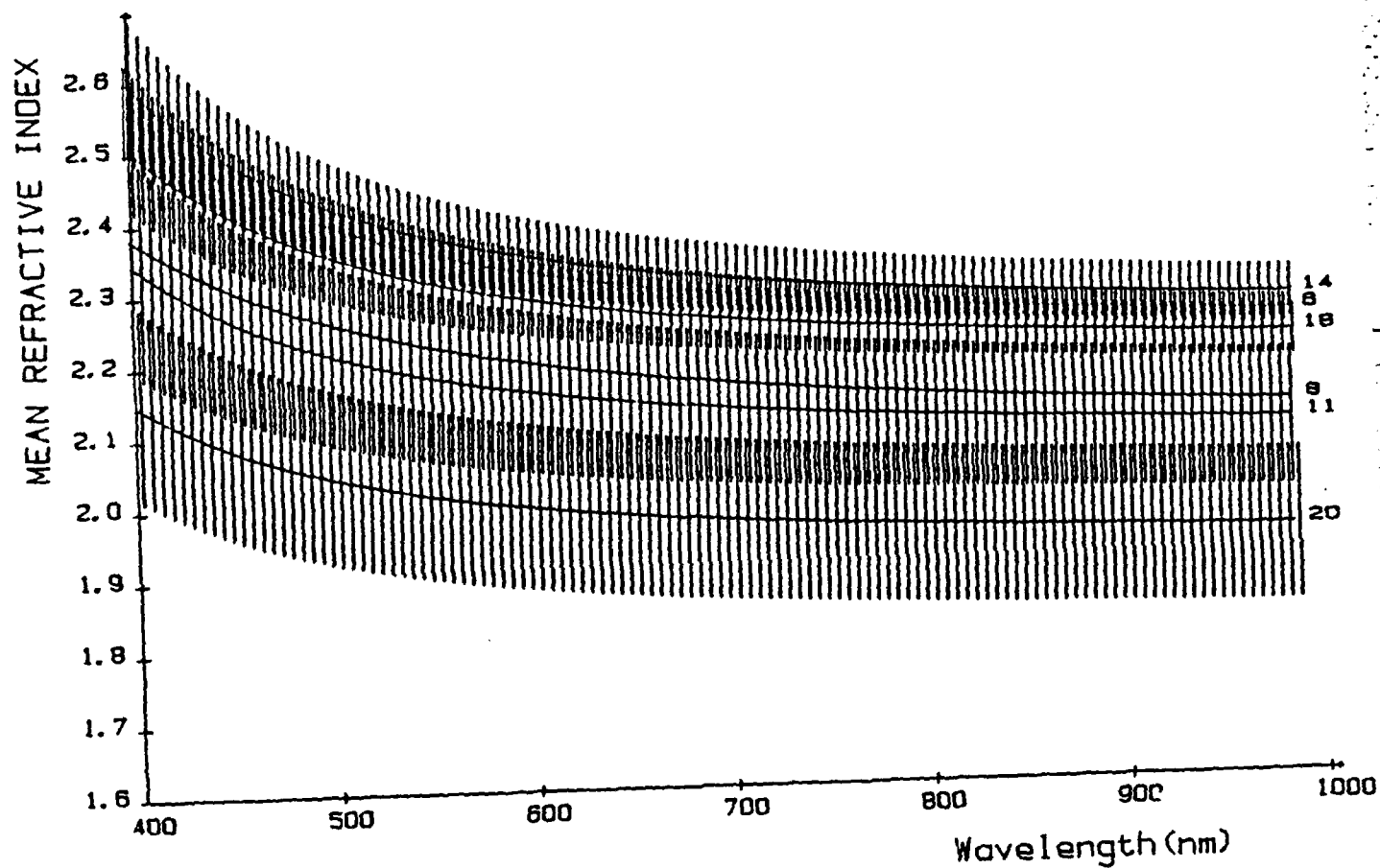


Figure 5. Difference between the mean values of the refractive indices measured in air and *in situ*.

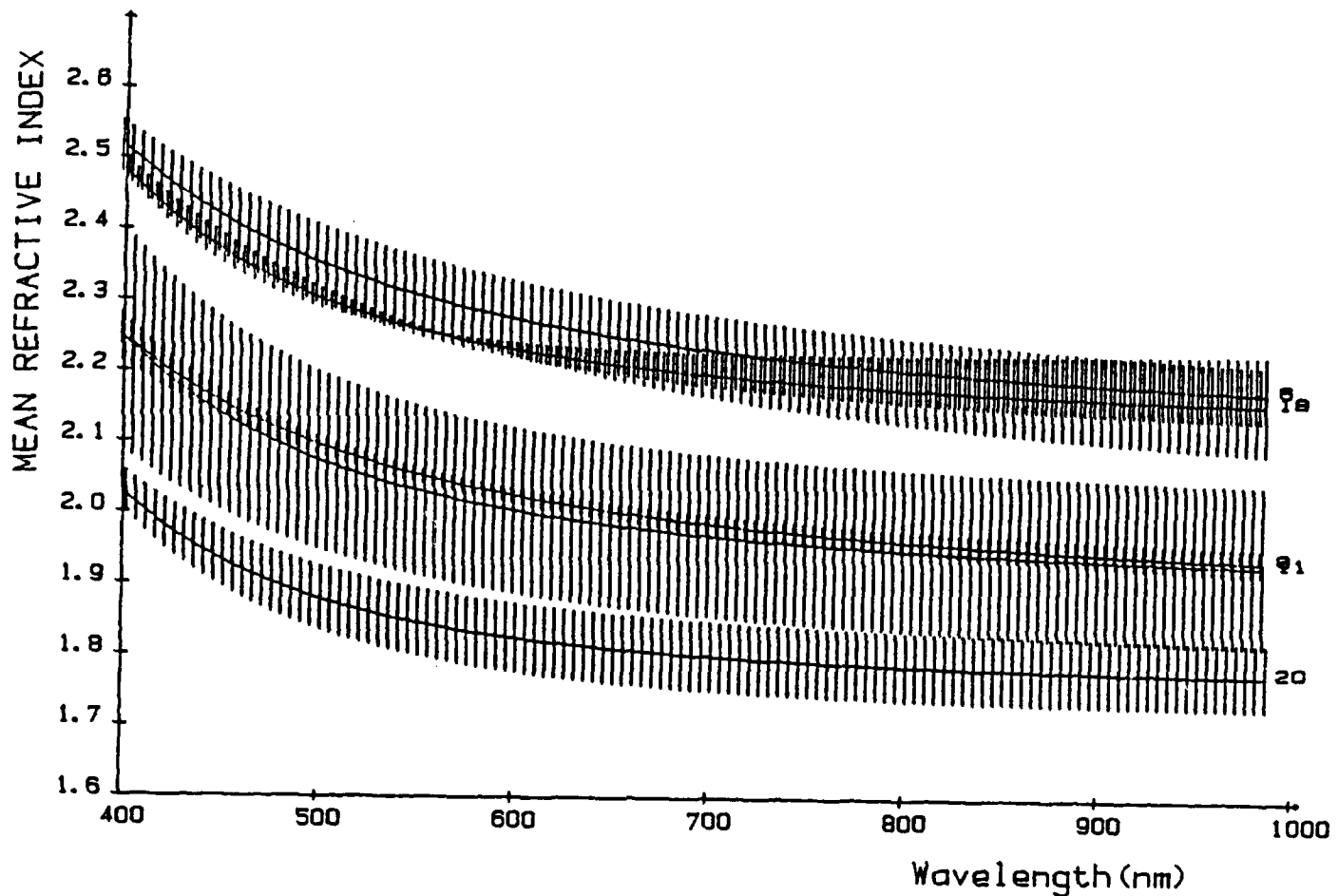
IN SITU MEASUREMENT



TITANIUM OXIDE (measurements in air)

Figure 4. Homogeneity defects of the layers referred to in figure 1.
 $\Delta n = n_{\text{inside}} - n_{\text{outside}}$ is plotted as a function of wavelength; the index systematically decreases from the substrate.

IN SITU MEASUREMENT



TITANIUM OXIDE (measurements during deposition)

Figure 3. The inhomogeneity Δn of titanium dioxide layers of fig. 1 calculated from *in situ* measurements during deposition; the index systematically decreases from the substrate.

IN SITU MEASUREMENT

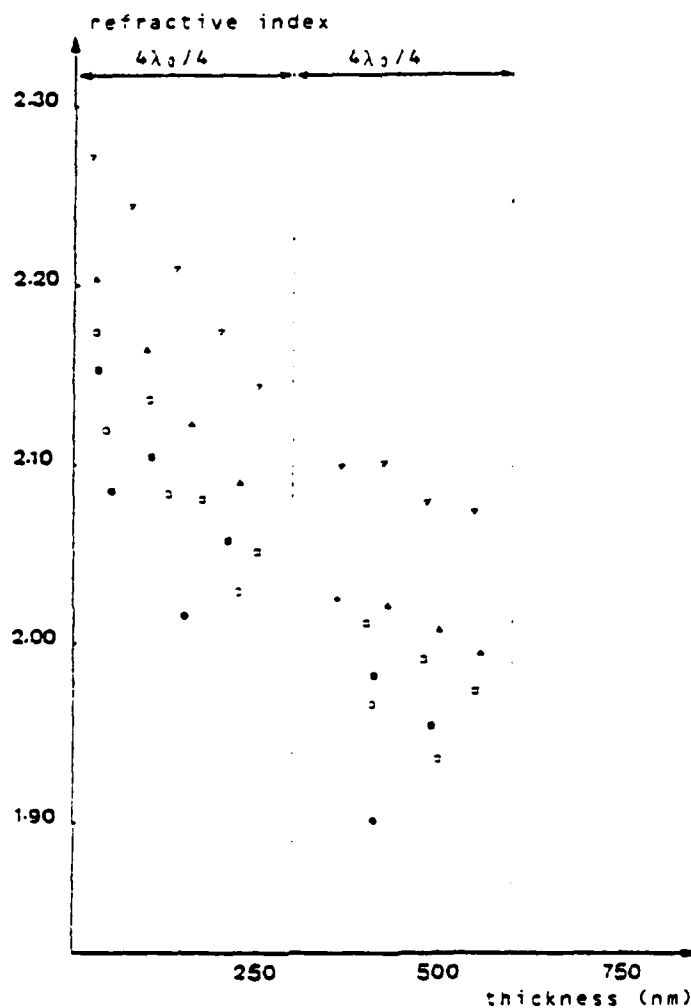


Figure 2. Titanium oxide. Values of refractive index as a function of thickness. The results are derived from the measurements recorded during the deposition for the wavelengths:

▽ 479.0nm ▲ 555.8nm □ 594.2nm ■ 632.6nm ○ 728.6nm
● 824.6nm

The optical thicknesses $4\lambda_0/4$ and $8\lambda_0/4$ are located on the thickness axis. ($\lambda_0 = 550$ nm)

IN SITU MEASUREMENT

APPENDIX 2: F J Van Milligen, B Bovard, M R Jacobson, J Mueller, R Potoff,
R L Shoemaker and H A Macleod
Development of an automatic scanning monochromator for
monitoring thin films
Submitted to Applied Optics, 1984

DEVELOPMENT OF AN AUTOMATED SCANNING MONOCHROMATOR
FOR MONITORING THIN FILMS

F.J. Van Milligen, Bertrand Bovard, Michael R. Jacobson,
James Mueller, Ross Potoff, Richard L. Shoemaker, H. Angus Macleod

University of Arizona
Optical Sciences Center
Tucson, Arizona 85721

ABSTRACT

A scanning monochromator system for the monitoring of thin film deposition in a box coater is described. The system employs data from both a quartz crystal oscillator and a wide band transmission spectrometer. The spectrometer uses a holographic grating as its dispersive element and a CCD array to collect the data. All data is sent to a microcomputer where the information is displayed, stored, and analyzed. Several applications, including measurement of optical constants of inhomogeneous films and characterization of moisture adsorption, are discussed.

1. INTRODUCTION

After an optical filter has been satisfactorily designed, it must be implemented in a production facility. For anything but the simplest of multilayer stacks, this involves the selection of the proper process parameters for a specific set of materials in a particular vacuum chamber. The length of time required to control this process fully depends upon the efficiency and fidelity of the monitoring techniques available to the operator. In general, there are two means of monitoring film deposition:

1) Optical monitoring: This technique is more appropriate in realizing coatings consisting of quarterwave layers by detecting the extrema of transmission or reflectance at a particular wavelength. This method is extremely stable for the control wavelength and only slightly less stable around it.¹ Therefore, it is used for coatings designed for performance over a narrow wavelength region.

2) Physical Mass Monitoring: By observing the natural resonance frequency of a quartz crystal, it is possible to determine the mass deposited on its surface; assuming densities for the film materials, one can compute the thickness of the layers. With this technique one can monitor layers of any thickness with high sensitivity. Unfortunately, since it does not include any measurements of the optical performance, it does not provide the stability of optical monitoring, and demands accurate calibration and reliable density data.

In this paper, we will describe a scanning monochromator system which employs both of these techniques in parallel with the added advantage of measuring the optical transmission of the sample over a wide wavelength range. We continue by discussing relevant features of the system and considering some of its applications.

2. IMPLEMENTATION

It is appropriate to begin by mentioning that our system was inspired by one built by the group led by Pelletier in Marseilles, France.^{2,3} Our scanning monochromator system was intended to augment the capabilities of a Balzers 760 box coater, which was delivered with an automated process controller (Balzers Model KB 101) based on a quartz crystal monitor and a second, unautomated, single wavelength optical monitor (Balzers Model GSM 210). The front end of the first subsystem was left intact; the second subsystem was replaced with our wideband optical monitoring portion of the scanning monochromator system.

Figure 1 is a descriptive flow diagram of the scanning monochromator system. To ensure that the signal reaching the CCD array is adequate, the original Balzers light source was replaced with a much brighter, 500 W tungsten-halogen lamp. This source met the required criteria: enough light to saturate the detectors and sufficient stability to rely on a single 100% reference line for an entire coating run. Unfortunately, its spectral profile, shown in Figure 2A, varies excessively and does not extend into the important

ultraviolet region. To solve this problem, we are currently replacing the tungsten-halogen with a xenon arc lamp which will have both a flatter spectrum and output in the ultraviolet, shown in Figure 2B.

Immediately adjacent to the source, the beam is modulated by a four sector chopper, which also provides a reference signal to the lock-in amplifier, part of the detector electronics beyond the detector. After the chopper, the light is projected by a lens into the chamber via a port in the baseplate, through the witness, or reference sample, and back out through a port in the chamber roof. For some experiments, a rotating fixture moves more than one sample through the monitor beam, permitting *in situ* coating comparisons. Figure 3 depicts the overall arrangement of the scanning monochromator with respect to the original box coater.

After exiting the chamber, the beam is turned by a flat mirror into the main scanning monochromator optics. First, it is refocused by a lens onto a slit, which is 1 cm high and approximately 30 μ m wide. After the slit, the beam encounters the dispersive element of the scanning monochromator, a Jobin-Yvon holographic, reflective grating, ruled at 300 lines/mm and designed to disperse light into a spectrum ranging from 400 to 800 nm, of which we use 440 to 800 nm due to our light source. The grating has sufficient optical power to image the slit onto the Fairchild 122 CCD array, which is reached after a final bounce from a flat folding mirror. The CCD intercepts the beam at an image of the grating's negative first order; the one-

inch long CCD array matches the one-inch flat field of the CCD at that point.⁴ A view of this part of the monochromator appears in Figure 4.

The CCD array consists of 1728 elements; our signal processing electronics averages sets of ten adjacent elements, providing us with 173 data points. These data levels are sent on to a dedicated IBM-PC, which records the data on five inch floppy disks and displays them on an Amdek video monitor for real time feedback to the plant operator. At the same time, information from the original process controller, based on the quartz crystal monitor, is sent through an interface module to the IBM-PC.

A flowchart showing how the computer handles the data appears in Figure 5. The IBM-PC incorporates a Tecmar A/D board, which accepts 12-bit data from both the quartz crystal monitor and the CCD array. Although the electronics are capable of running at a rate of four spectra per second, we generally take one spectrum every three seconds. This is quite adequate, since at our typical deposition rates (primarily of oxides), we deposit ten to twenty Angstroms of material in three seconds. The potential for data rates at least an order of magnitude higher would permit us to monitor extremely rapid changes, should the need arise. Table 1, below, summarizes important characteristics of the scanning monochromator monitor.

Before each run, wavelengths are calibrated by inserting a piece of didymium glass in the light path and then setting zero readings in the data to the didymium's known absorption lines. For

readings other than those given by the absorption lines the wavelength is determined by linear interpolation between known points. We estimate an accuracy of 2 to 4 nm over the range we have tested with available spectral line sources.

3. APPLICATIONS

Several examples of applications for the scanning monochromator monitor follow:

1) A sequence of transmission spectra for each run can be stored for later analysis of the effects of various process parameters. A 360K double-density 5.25 inch disk can accommodate about 50 minutes of continuously monitored spectral data.

2) The wideband transmission spectra that appear on the monitor provide the plant operator with a much broader view of coating progress; should problems arise, the operators can base their decisions during deposition on a larger data base.

3) Monitoring done *in situ* permits testing and observation of coatings without removing them from the system. One example of this feature's utility appears in Figure 6: It examines the effect of water adsorption on a filter. ⁵

4) The larger data base available to the computer permits better characterization of a film's optical constants. Figure 7 shows one such calculation for a film of TiO_2 as it grows. We note that this illustrates the dispersion of n and k with thickness at a particular wavelength. The system can also derive the dispersion with wave-

length at a particular thickness. ⁶

4. ACKNOWLEDGMENTS

The development of our scanning monochromator system was inspired by a pioneering system constructed at the Laboratoire d'Optique de l'Ecole Nationale Supérieure de Physique in Marseille, France, led by E. Pelletier and including F. Flory, A. Fornier, and R. Richier. One other member of that group is among the authors of this paper; we were fortunate enough to have B. Bovard as a post-doctoral scientist for one year at the Optical Sciences Center. His visit had an extremely stimulating influence on the construction and completion of the instrument. The Air Force Office of Scientific Research [AFOSR] provided salary support for his year in Arizona. We would also like to thank T. D. Ferguson and Russell Chipman of the Optical Sciences Center for their helpful discussions. M. Osgood skillfully executed the figures. We also would like to thank the Defense Advanced Research Projects Agency [DARPA] for their generous support of basic thin films research through a three-year contract monitored by the Naval Weapons Center.

5. REFERENCES

1. H.A. Macleod, "Turning Value Monitoring of Narrow-Band All-Dielectric Thin Film Optical Filters, " *Optical Acta*, **19**, 1-23 (1972).
2. P. Bousquet and E. Pelletier, "Optical Thin Film Monitoring - Recent Advances and Limitations," *Thin Solid Films*, **77**, 165-79 (1981).
3. B. Vidal, A. Fornier, and E. Pelletier, "Wideband Optical Monitoring of Non-Quarterwave Multilayer Filters," *Applied Optics*, **18**, 22, 3851-56 (1979).
4. J.M. Lerner, J. Flamand, J.P. Laude, G. Passereau, and A. Thevenon, "Diffraction Gratings Ruled and Holographic - A Review," *SPIE* **240**, 82-88 (1980).
5. S.G. Saxe, M.J. Messerly, B. Bovard, L. Desandre, F. J. Van Milligen, and H.A. Macleod, "Ion Bombardment-Induced Retarded Moisture Adsorption in Optical Thin Films," *Applied Optics*, **23**, 20, 3633-3637 (1984).
6. B. Bovard, S.G. Saxe, M.J. Messerly, F.J. Van Milligen, and H.A. Macleod, "Techniques for Thin-Film Optical Constant Derivation from In Situ Transmission Measurements," presented at the OSA 1984 Annual Meeting, San Diego, California, October 29 - November 2, 1984.

TABLE 1: SYSTEM PERFORMANCE

Wavelength Range	440 - 800 nm
Wavelength Resolution	2 nm
Resolving Power	300
Etendu of System	$1 \times 10^{-3} \text{ cm}^2\text{-sr}$
Minimum Transmission	2%
Signal Level of CCD	70% of saturation at 650 nm

FIGURE CAPTIONS

1. Scanning Monochromator Flow Diagram
- 2a. Spectral Profile of Tungsten Halogen Lamp
- 2b. Spectral Profile of Xenon Arc Lamp
3. Appearance of Scanning Monochromator system
4. Top view of Scanning Monochromator
5. Flowchart of Computer Data Handling Program
6. Example of Water Adsorption in a TiO_2 , SiO_2 Fabry-Perot Filter
7. Variation of optical constants of TiO_2 as the film is being deposited. Upper curve corresponds to n , lower curve to k .

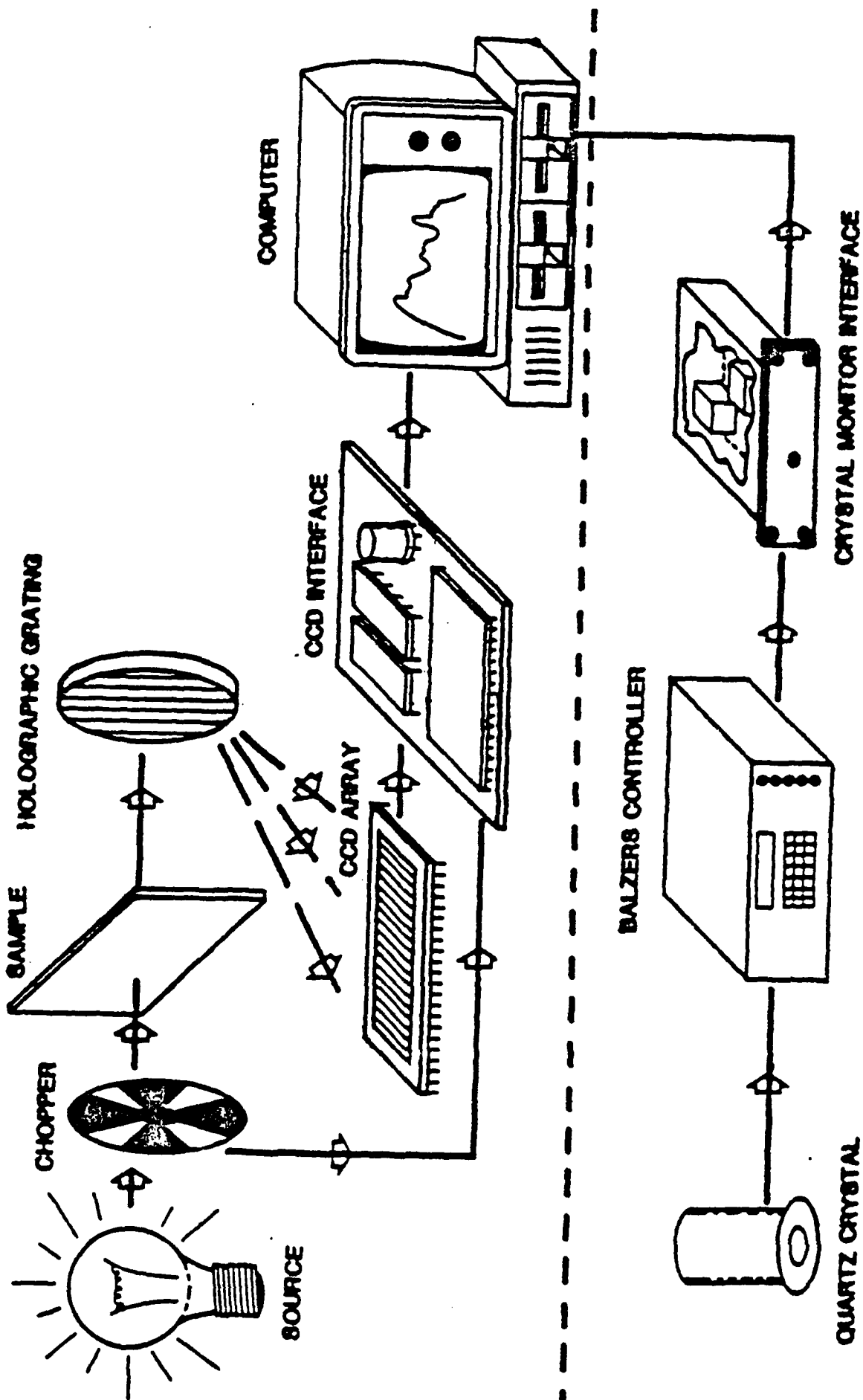


Fig 1. Scanning Monochromator Flow Diagram.

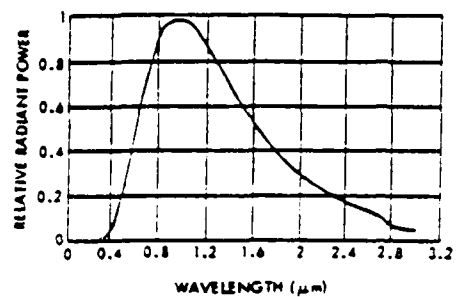


Fig 2a. Spectral Profile of Tungsten Halogen Lamp.

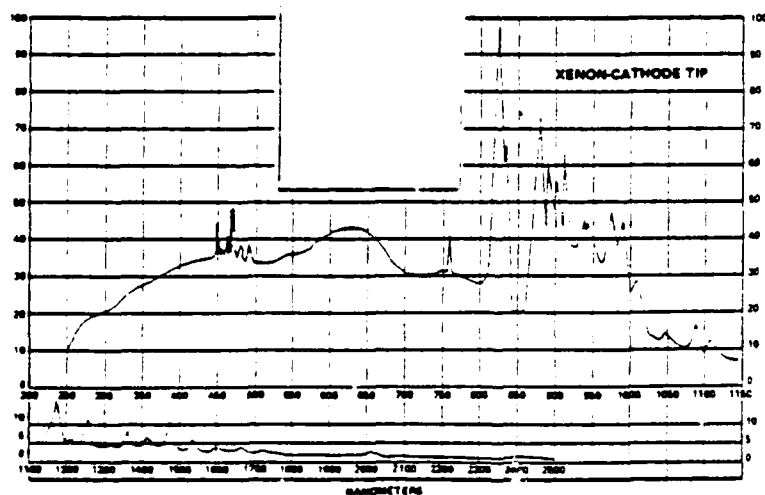


Fig 2b. Spectral Profile of Xenon Arc Lamp.

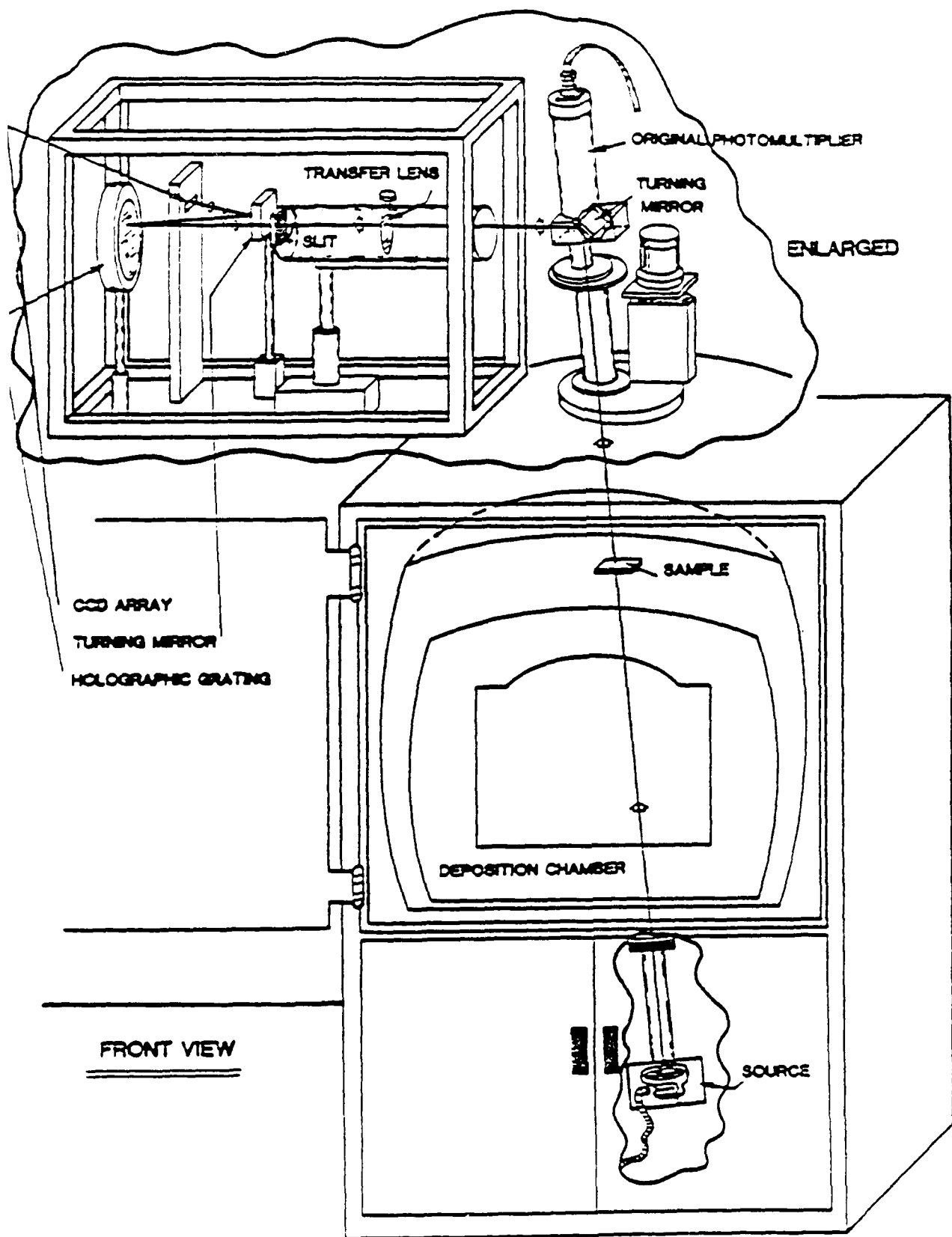


Fig 3. Appearance of Scanning Monochromator system.

III. Data Processing and Simulation

The envelope computation requires an accurate knowledge of the extrema together with a method to fit curves to these points. It was thought possible that the data processing used for the calculation of the envelopes might introduce a bias in the results given by the program of optical constant determination. However, we are able to show that it is not the case so that our results are free from such effects.

III. 1. Smoothing the curve of transmission versus time

Many methods are available for smoothing, but our major concern is to smooth without distorting the curve. For this reason, we decided to use a filtering method based on a finite impulse response filter calculated to have a linear phase and an extremely flat low-pass band. We thus avoid any distortion introduced by a nonlinear phase and the attenuation due to a nonflat passband. The filter does still introduce a delay equal to the derivative of its phase versus frequency, but this delay is constant and is corrected in the computation by an entire shift of the curve. Details of this type of approach are given in (9) which inspired the present design and so we limit our description to demonstrating its application to a real signal in Figs. 1 and 2.

III. 2. Envelope Computation

The equations of the envelopes are computed by segments. The first group of three points gives a parabola which is used to describe the segment of the curve between the first two points. Next the first point is discarded and replaced by the fourth point. A new parabola is now

II.2. Stability of deposition and conclusion

Provided we know the envelopes of a curve of transmission, using these analytical expressions we are able to derive the optical constants. But the necessity of knowing the envelopes as functions of thickness leads us to a very basic assumption concerning the stability of growth of the layer. The envelopes calculated using the measured transmission versus time are usable if they do not shift during the deposition process, which means that an earlier part of the layer is not modified during the deposition of a later part.

It is easy to foresee the importance of having an accurate way of determining extrema of the transmission curves. Their precise estimation, both value and position, demanded that we consider some numerical treatments of the raw data before calculating the envelopes fitting these points. We present in the next section the data processing techniques developed together with a justification of their validity and of the expressions presented above.

since calculation of $\frac{1}{d} \int_0^d n(z)dz$ is impossible, we make an

approximation and write that $\bar{n} = \frac{1}{t} \int_0^t n(u)du$ where t is the instant

when the extremum occurs.

This is equivalent to assuming that the rate of deposition (change in thickness per unit time) is constant. The assumption is reasonable because our deposition rate is automatically controlled.

With regard to the profile of extinction coefficient we note first that a mean value of the extinction coefficient can be derived each time we reach a new quarterwave:

$$\bar{k} = -\frac{\lambda}{4\pi d} \text{Log } \alpha(d) \text{ with } \alpha(d) = \frac{C_1[1-(T_{\max}/T_{\min})^{1/2}]}{C_2[1+(T_{\max}/T_{\min})^{1/2}]} = \exp\left(-4\pi \frac{\bar{k}d}{\lambda}\right)$$

but since the function α is available at any instant during the growth of the layer, we can also calculate its derivative versus time and obtain an expression giving the profile of extinction coefficient.

$$k(z) = -\frac{\lambda}{4\pi} \frac{1}{\alpha(z)} \frac{d\alpha}{dz} \text{ where } z \text{ is the thickness of the layer.}$$

Because of the derivative, this expression presents some sensitivity to errors but can still be used to obtain an indication of the absorption of the material.

refractive index, the geometrical thicknesses and the extinction coefficient profile.

The expression of the innermost refractive index is obtained assuming n_{in} = n_{out} and $d = 0$ so that:

$$n_{in} = [N + (N^2 - n_o^2 n_s^2)^{1/2}]^{1/2} \text{ where } N = \frac{n_o^2 + n_s^2}{2} + 2n_o n_s \left(\frac{T_{max} - T_{min}}{T_{max} + T_{min}} \right)$$

The expression of the outermost refractive index is then:

$$n_{out} = \frac{2n_{in}n_s n_o}{n_{in}^2 - n_s^2} \frac{T_{max} - T_{min}}{T_{max} + T_{min}} + n_o \left[1 + 4n_{in}^2 n_s^2 \left(\frac{T_{max} - T_{min}}{T_{max} + T_{min}} \right)^2 / (n_{in}^2 - n_s^2)^2 \right]^{1/2}$$

which is calculable only if we know the innermost index value.

Provided we assume the innermost index is stable we can calculate the profile of the refractive index of an inhomogeneous layer. Note that it requires the knowledge of the substrate refractive index, which can be measured independently, but it does not require the value of wavelength.

We also require the geometrical thickness. Since we are dealing with low-absorption materials, the extrema of transmission occur when the optical thickness of the layer is a multiple of a quarterwave.

If m is the order of the extremum ($m=1$ indicating the first minimum) the corresponding geometrical thickness is

$$d = m \frac{\lambda}{4\bar{n}} \text{ where } \bar{n} = \frac{1}{d} \int_0^d n(z) dz$$

$$T = \frac{16n_s n_o n_{in} n_{out} e^{2\delta_2}}{C_1^2 + C_2^2 e^{4\delta_2} + 2C_1 C_2 e^{2\delta_2} \cos 2\delta_1}$$

$$\text{where } C_1 = (n_{out} + n_o)(n_s + n_{in}) \quad C_2 = (n_{out} - n_o)(n_s - n_{in})$$

$$\delta_1 = 2\pi n d / \lambda$$

$$\delta_2 = -2\pi k d / \lambda$$

In the following we shall assume that we are dealing with a high index layer so that C_2 is negative. Then the two expressions of the envelopes become:

$$T_{\max} = \frac{16n_o n_s n_{in} n_{out} e^{2\delta_2}}{(C_1 + C_2 e^{2\delta_2})^2}$$

$$T_{\min} = \frac{16n_o n_s n_{in} n_{out} e^{2\delta_2}}{(C_1 - C_2 e^{2\delta_2})^2}$$

These two equations are used to determine the outermost index for each instant during film deposition. They are also used to calculate the extinction coefficient at the quarterwave points.

However, all these derivations are possible only if we make a very basic assumption about the stability of the layer during deposition. This assumption is simply that the innermost index does not vary during the growth of the film. The profiles of the optical constants can then be derived and considered as functions of thickness instead of time.

We shall not go through the details of the derivation and we shall only give the analytical expressions for the innermost and outermost

A non-absorbing inhomogeneous layer, provided it is reasonably thick and there is appreciable index contrast at its boundaries, can be represented by the characteristic matrix⁸:

$$\begin{bmatrix} (n_{in}/n_{out})^{1/2} \cos \delta & i \sin \delta / (n_{out} n_{in})^{1/2} \\ i(n_{in} n_{out})^{1/2} \sin \delta & (n_{out}/n_{in})^{1/2} \cos \delta \end{bmatrix} \quad (8)$$

where n_{out} is the index at the outer surface of the film

n_{in} is the index at the inner surface of the film, and

δ is the phase thickness.

If we assume that the absorption is very small, the same matrix can be used with the extinction coefficient included in δ only so that

$$\delta = 2\pi(\bar{n} - i\bar{k})d/\lambda$$

where \bar{n} is the mean index of the film (i.e. $\bar{n} = \frac{1}{d} \int_0^d n(z)dz$),

\bar{k} is the mean extinction coefficient (i.e. $\bar{k} = \frac{1}{d} \int_0^d k(z)dz$),

λ is the wavelength and

d the thickness of the layer.

Let us assume that the incident medium has a refractive index n_0 and that the substrate is nonabsorbant of index n_s . After some tedious calculation, we find the expression for the transmission of the coated substrate:

In the case of negligible extinction coefficients the derivation of the refractive index can be achieved using an admittance circle method based on transmission measurements during the growth of the layer⁵. But since our interests lie more in slightly absorbant materials such as oxides, we have developed a technique inspired by the envelope method described by Manifacier et al (6). We have used an inhomogeneous model of a thin film to derive the refractive index and the extinction coefficient profiles.

II.1. Envelope method in the inhomogeneous case

Manifacier et al⁶ have fully described the envelope method in the limiting case of an homogeneous thin film where only transmission measurements are required for the derivation of n and k . A generalization to an inhomogeneous model was presented by Arndt et al⁷ to derive the optical constants from measurements of reflectance and transmittance. In these studies reflection and transmission are considered as functions of wavelength and their envelopes are used to calculate the optical constants. To obtain the profiles of the optical constants, as in this study, we considered the envelopes of the curve of transmittance as functions of thickness for a chosen wavelength. We were able to obtain the dispersion by applying the same method to a range of wavelengths.

We now demonstrate the principle of the method and give the analytical expressions for the optical constants.

I. Introduction

The refractive index and the extinction coefficient of a thin film depend upon the conditions of deposition and as a consequence upon the structure of the film itself. In the case of oxides, inhomogeneities are largely due to the film's columnar structure¹ and to the variations in degree of oxidation throughout the layer. The derivation of their profiles as a function of thickness is difficult once the layer has been deposited. Furthermore, most techniques developed to measure the refractive index are carried out under atmospheric conditions. Exposure of a film to the air modifies its optical properties: the voids existing in its structure tend to adsorb moisture and an oxidation process may occur for a suboxidized layer, changing the refractive index and the extinction coefficient.^{2,3} Therefore a technique taking into account the evolution of the transmission of a layer growing in vacuo has great advantages. To achieve such measurements we have used a scanning monochromator system⁴ which provides us with the transmission over the visible spectrum versus time, during deposition. Using these values we have developed a technique for deriving the profiles of the optical constants. After a verification of the optical constants determination technique by computer simulation, we have applied the method to various layers of titanium dioxide. This technique can then be used as a means of monitoring the effect on the optical constants of a change in any of the parameters used for the coating process.

II. Determination of the profile of the optical constants of an inhomogeneous film

Optical Constants derivation for an inhomogeneous
thin film from in situ transmission measurements

B. Bovard, F.J. Van Milligen, M.J. Messerly, S.G. Saxe, H.A. Macleod

University of Arizona
Optical Sciences Center
Tucson, Arizona 85721

ABSTRACT

The optical constants of a thin film depend upon the structure of the film itself. A technique, based on transmission measurements carried out in vacuo, has been developed to derive the profiles of the refractive index and extinction coefficient. The interpretation of the profiles gives information on the layer structure in vacuo. The technique can be used as a means of monitoring the variations of the optical constants with changes in the deposition parameters. This paper presents the technique, which is based on an envelope method, and gives some experimental results.

IN SITU MEASUREMENT

APPENDIX 3: B Bovard, F J Van Milligen, M J Messerly, S G Saxe and H A Macleod

Optical constants derivation for an inhomogeneous thin film
from in situ transmission measurements
Submitted to Applied Optics, 1984

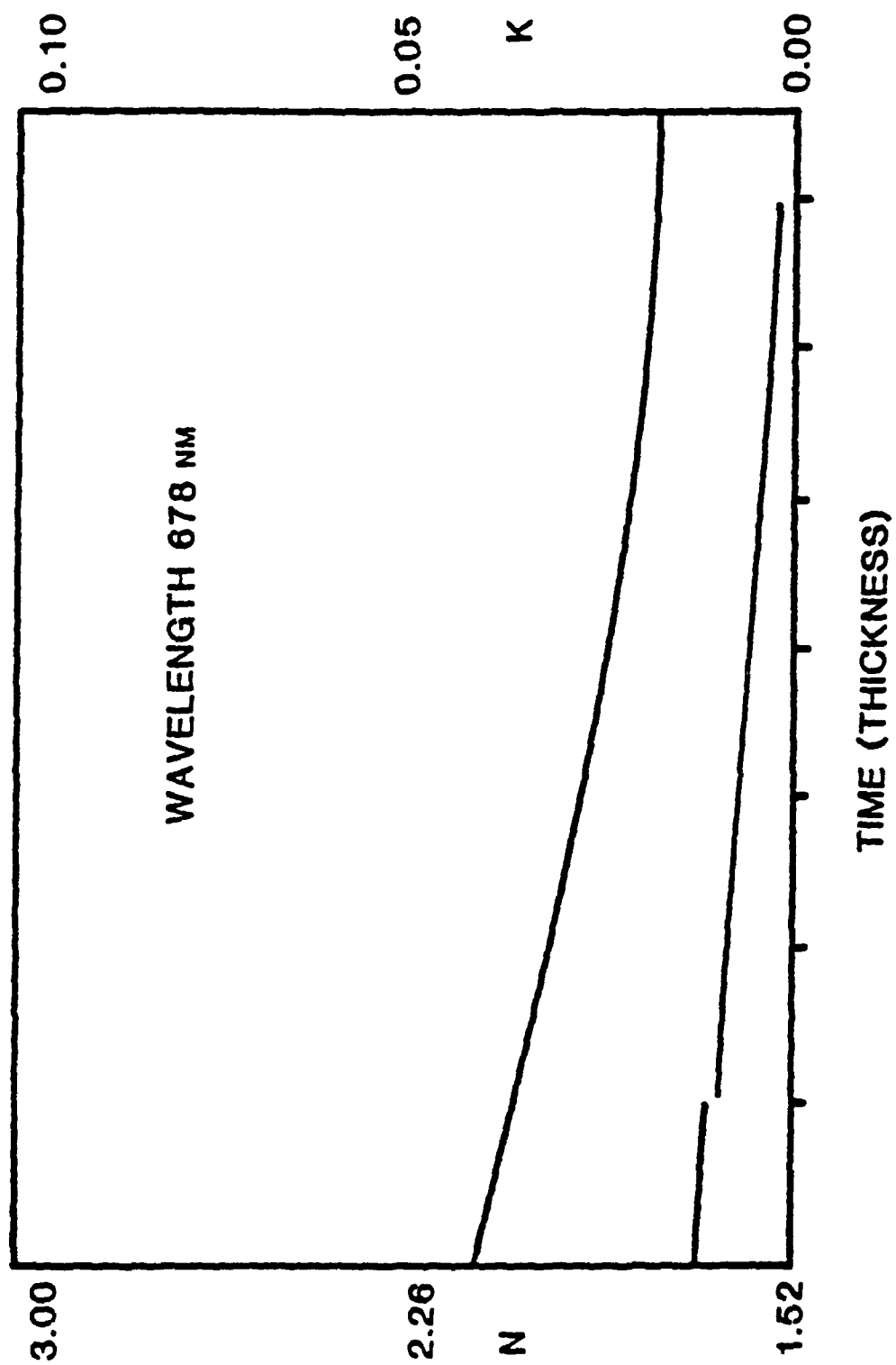


Fig 7. Variation of optical constants of TiO_2 film as the film is being deposited.
Upper curve corresponds to n, lower curve to k.

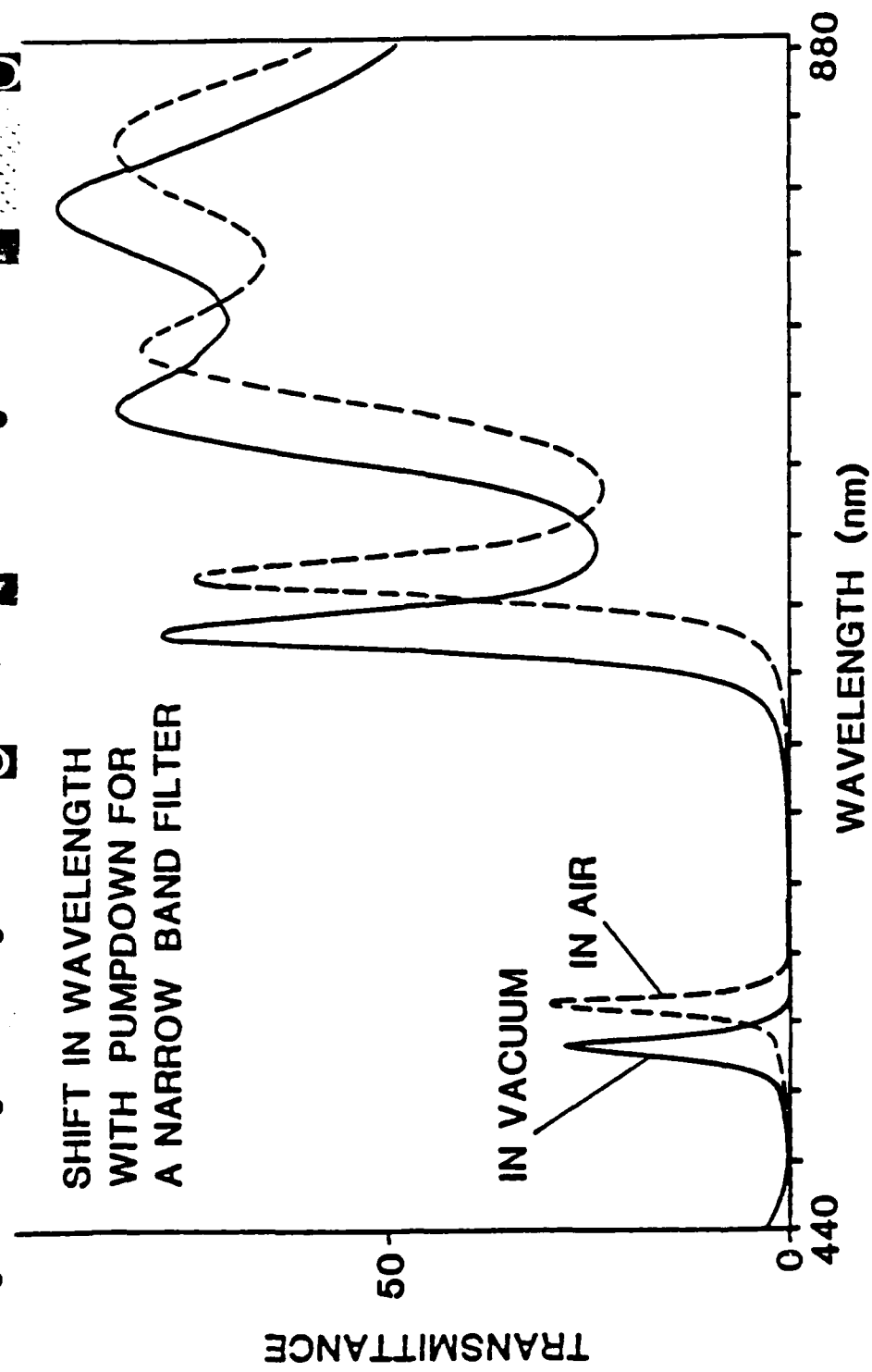


FIG. 6. Example of Water Adsorption in a TiO_2 , SiO_2 Fabry-Perot Filter

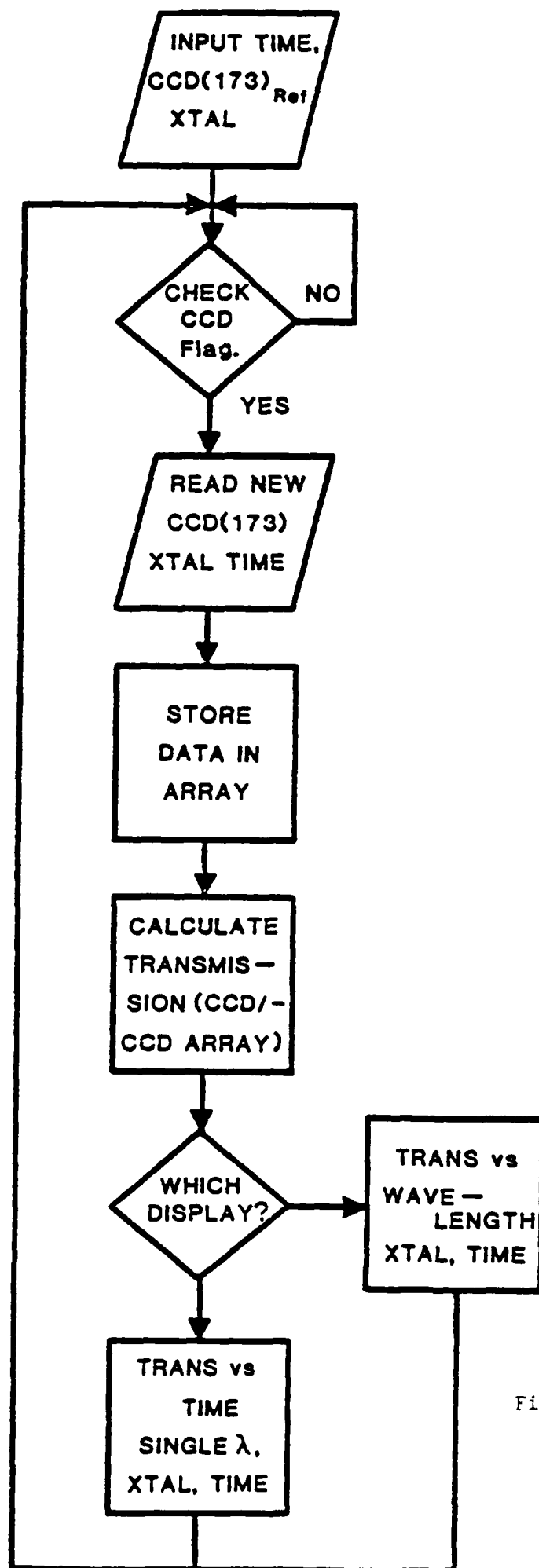


Fig 5. Flowchart of Computer Data Handling Program.

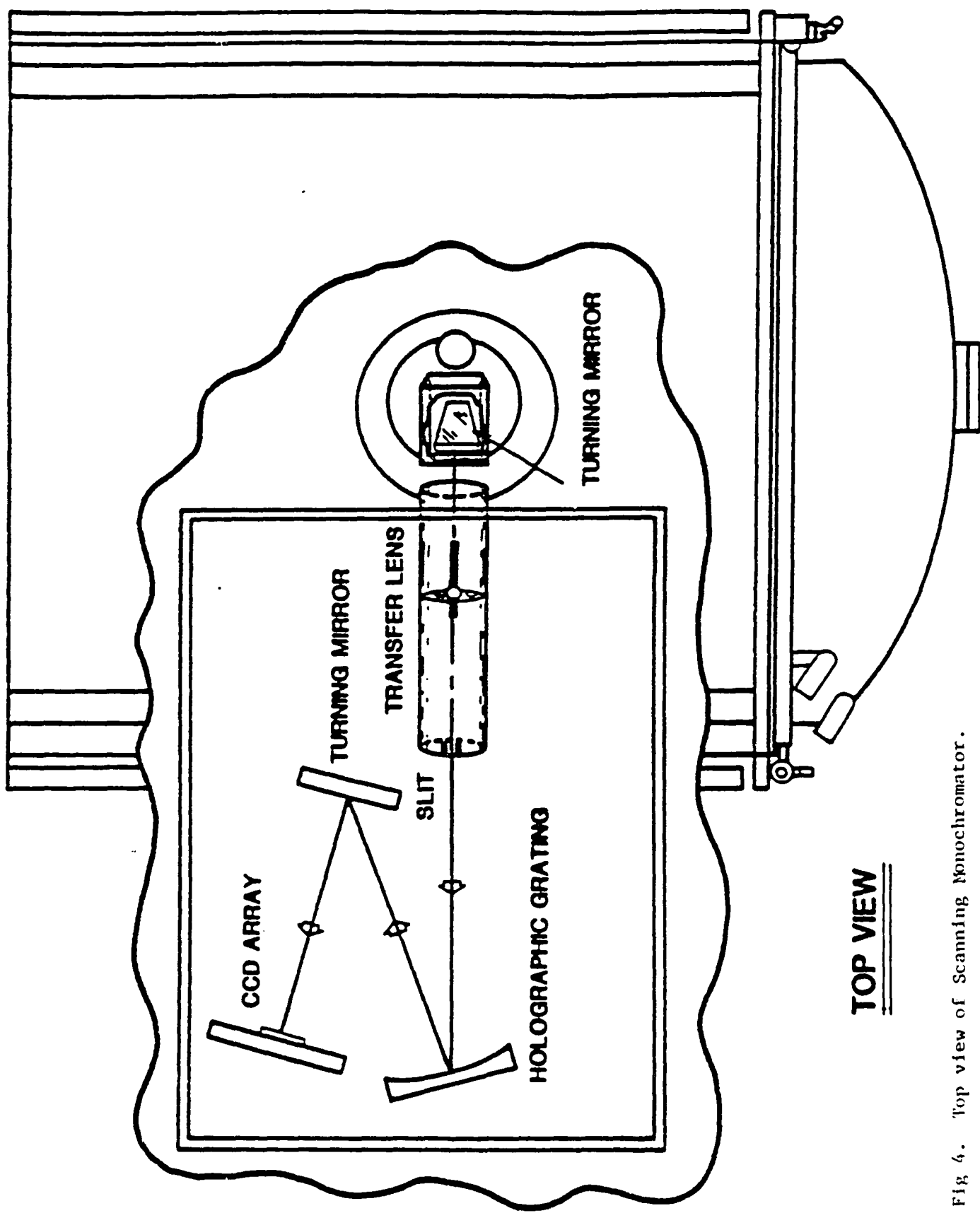


Fig 4. Top view of Scanning Monochromator.

calculated and used to describe the segment between the second and third points. This operation is repeated until the entire curve is produced.

III. 3. Verification and precision of the technique

The validity of the expressions for the refractive indices and the extinction coefficient has been checked by some simulations, the results of which are presented here.

A program able to handle variable optical constants has been developed to compute the evolution of the transmission of a coated substrate during growth of a thin film. The profiles of the optical constants are fed into the program which divides the inhomogeneous layer into a stack of homogeneous sublayers each of thickness 1 nm . The transmittance is then recorded on disk files exactly as when the scanning monochromator is used. The optical constant determination program is then used to compute the index and estimation coefficient profiles. Their comparison with the original ones verifies the accuracy of the technique. Our goal was also to show it is possible to separate the inhomogeneity of the refractive index from the extinction coefficient. Of the many computations that have been performed we simply show two of the most characteristic ones.

The simplest case is that of a homogeneous layer. Taking starting values of $n = 2.3$ and $k = 10^{-3}$, the optical constants were calculated for two wavelengths 400 and 800 nm and the indices found were to be within 0.03% of the initial value. As foreseen, the efficiency of the

calculation of the extinction coefficient was not as good, leading to a 10% relative error.

To test the derivation in the case on an inhomogeneous layer, an arbitrary curve of refractive index was chosen to compute the evolution of transmission : $n(d) = 2 + 0.3 \exp(-d/200)$ where d is the thickness of the layer. The extinction coefficient was assumed constant equal to 10^{-1} . Table 1 shows the calculated results for two wavelengths. The columns $\Delta n_{in}/n_{in}$ etc. list the error in the determination expressed as a percentage.

TABLE 1

Wavelength						
(nm)	n_{in}	$\Delta n_{in}/n_{in}$	n_{out}	$\Delta n_{out}/n_{out}$	k	$\Delta k/k$
400	2.297	0.15%	2.012	0.09%	1.03×10^{-3}	7%
800	2.283	1%	2.025	0.7%	$0-1.7 \times 10^{-3}$	-

Results of simulation calculations

These results indicate that we can expect acceptable accuracy in the refractive index profile using this technique. It is important to note that the higher accuracy corresponds to the shorter wavelength. This is due to the greater number of extrema at the shorter wavelength, which provides more information so the envelopes calculated have a more exact position. This inaccuracy of the envelopes leads to questionable values of extinction coefficient for the longer wavelength. These results are rigorously true only for the cases considered but they strongly suggest what we can generally expect from this method. The relative accuracy of the refractive index depends also upon the quality of the transmittance measurements: it ranges from $\Delta T/T$ to $5\Delta T/T$ where $\Delta T/T$ is the relative accuracy achieved in the transmittance measurements.

IV. Experimental results

The optical constant determination has been carried out for titanium dioxide layers only. We will present the results obtained with two different layers, the first layer fitting the model used in this derivation and the second being unstable.

The starting material used in our experiments was Ti_2O_3 , evaporated by electron bombardment onto a glass substrate.

For the first layer we consider, the oxygen partial pressure was 4.4×10^{-4} mbar and the chamber temperature varied from 204° to $227^\circ C$ during the deposition.

The profile of refractive index and of extinction coefficient are plotted in Fig. 3 for the wavelength 678 nm. The thickness of the layer is 670 nm, the inner index is 2.135 and the outermost index 1.794. The layer is inhomogeneous, as expected for an oxide layer, and slightly absorbant.

The correlation between index and extinction coefficient can be interpreted as an increase of the degree of oxidation with the thickness of the layer and as a decrease of the packing density due to a conical form of the columnar structure. It is difficult to choose which has the primary effect.

Fig. 4 gives the dispersion of the innermost and outermost refractive indices. A high dispersion for the outermost index suggests a more absorbant outer part of the layer.

The layer appears to be stable and therefore our results indicate that it is an inhomogeneous layer showing a decrease in its packing density and a decrease in its oxidation degree in the direction of growth.

We now examine an unstable layer. This layer was deposited in a chamber at a temperature of 260°C in the presence of oxygen at a partial pressure of $1.3 \cdot 10^{-4}$ mbar.

This atmosphere was intentionally deficient in oxygen compared with the usual conditions for the deposition of titanium dioxide and we expected some absorption in the layer. We are not disappointed as shown Fig. 5

but furthermore another phenomenon seems to occur. The curve of the extinction coefficient falls with thickness towards a value which could even become negative. This is almost certainly the effect of instability in the oxidation of the layer: starting with a high deficiency of oxygen the inner part of the film is gradually oxidized as the layer grows. This defeats the technique presented here since the extrema used to calculate the envelopes are changing with the oxidation of the layer and also because we have assumed the innermost refractive index to be constant. The real curve is impossible to obtain but we can expect that it would present a less inhomogeneous profile.

Other experiments have been carried out to understand the limitations of this method. The instability of the layer can manifest itself by the occurrence of negative extinction coefficients, by thicknesses varying with wavelength or by very misshapen profiles of index. Nevertheless, the application of this technique to stable layers gives very interesting results. These can give information on the structure of the layer in terms of packing density as well as in terms of degree of oxidation. It is also important to know that layers can be unstable and to be able to recognise such an instability. Further work is required in this area. We hope that eventually it may be possible to distinguish an instability caused by a structural rearrangement from a reoxidation of some innermost portions of the film.

V. Conclusion

This method has been developed for layers presenting a high index, a small homogeneity, and a small extinction coefficient. It permits the determination of the profiles of the optical constants and the dispersion of index in vacuo provided the assumption of stability is fulfilled. It identifies layers that are unstable. It makes possible the study of the variations of the optical constants with changes in the deposition parameters.

Major support for this work was provided by the Defense Advanced Research Projects Agency (DARPA) through a contract with the Naval Weapons Center, China Lake. Additional support was also given by DARPA through a contract with the Naval Ocean Systems Center, San Diego. Bovard was supported by the Air Force Office of Scientific Research and Saxe by a fellowship from the U.S. Army Research Office.

References

1. H.A. Macleod. "Microstructure of optical thin films." Proc SPIE 325 pp21-28 (1982).
2. Cheng-Chung Lee. "Moisture adsorption and optical instability in thin film coatings." Ph.D. dissertation, University of Arizona (1983).
3. J. P. Borgogno, P. Bousquet, F. Flory, B. Lazarides, E. Pelletier and P. Roche. "Inhomogeneities in films: limitation of the accuracy of optical monitoring of thin films." Applied Optics 20 pp90-94 (1981).
4. F. Van Milligen, B. Bovard, M.R. Jacobson, J. Mueller, R. Potoff, H.A. Macleod, R. Shoemaker, University of Arizona. "Development of an Automated Scanning Monochromator for a Balzers 760 Evaporation System." Paper presented at OSA Annual Meeting, San Diego, October 1984.
5. B. Schmitt, Thèse de docteur ingénieur "Problèmes de réalisation des filtres spectraux multidiélectriques: contrôle simultané de l'indice de réfraction et de l'épaisseur des couches en cours de formation." Ecole Nationale Supérieure de Physique, Marseille (1983).
6. J.C. Manifacier, J. Gasiot, J.P. Fillard. "A Simple method for the determination of the optical constants n , k and the thickness of a weakly absorbing thin film." Journal of Physics E: Scientific Instruments, 9 pp1002-4 (1976).
7. D.P. Arndt, R.M.A. Azzam, J.M. Bennett, J.P. Borgogno, C.K. Carniglia, W.E. Case, J.A. Dobrowski, U.J. Gibson, T. Tuttlehart,

F.C. Ho, V.A. Hodgkin, W.P. Klapp, H.A. Macleod, E. Pelletier, M.K.

Purvis, D.M. Quinn, D.H. Strome, R. Swenson, P.A. Temple, T.F.

Thoun. "Multiple Determination of the Optical Constants of Thin Film Coating Materials." *Applied Optics*, 23 pp3571-3596 (1984)

8. R. Jacobsson. "Inhomogeneous and coevaporated homogeneous films for optical Applications." *Physics of Thin Films*, ed. G. Hass, M.H. Francombe and R.W. Hoffman, 8 pp51-98 Academic Press (1975).
9. S.M. Bozic. "Digital and Kalman Filtering. An Introduction to Discrete Time Filtering and Optimum Linear Estimation." Edward Arnold, London (1979).

FIGURE CAPTIONS

1. Plot of noisy signal. The extrema are difficult to determine with accuracy.
2. After filtering, the extrema have been extracted from the noise without distorting or attenuating the transmission curve.
3. Profile of refractive index and extinction coefficient for a stable titanium dioxide layer. (Upper curve represents n , lower curve k).
4. Dispersion of innermost and outermost refractive index for a stable layer of titanium dioxide.
5. Example of result given by the method when applied to an unstable layer. Titanium dioxide layer deposited in an oxygen deficient atmosphere.

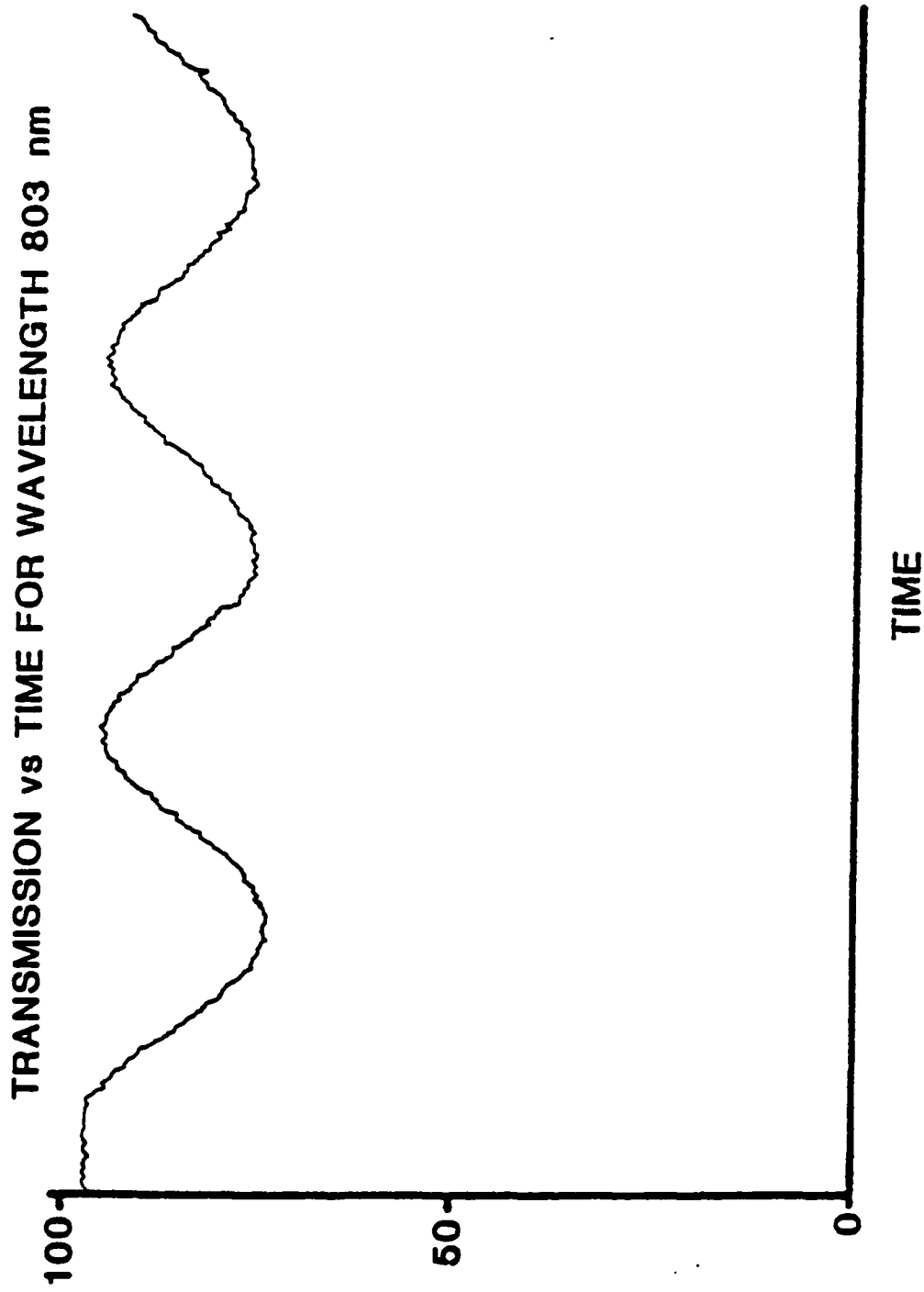


Fig 1. Plot of noisy signal. The extrema are difficult to determine with accuracy.

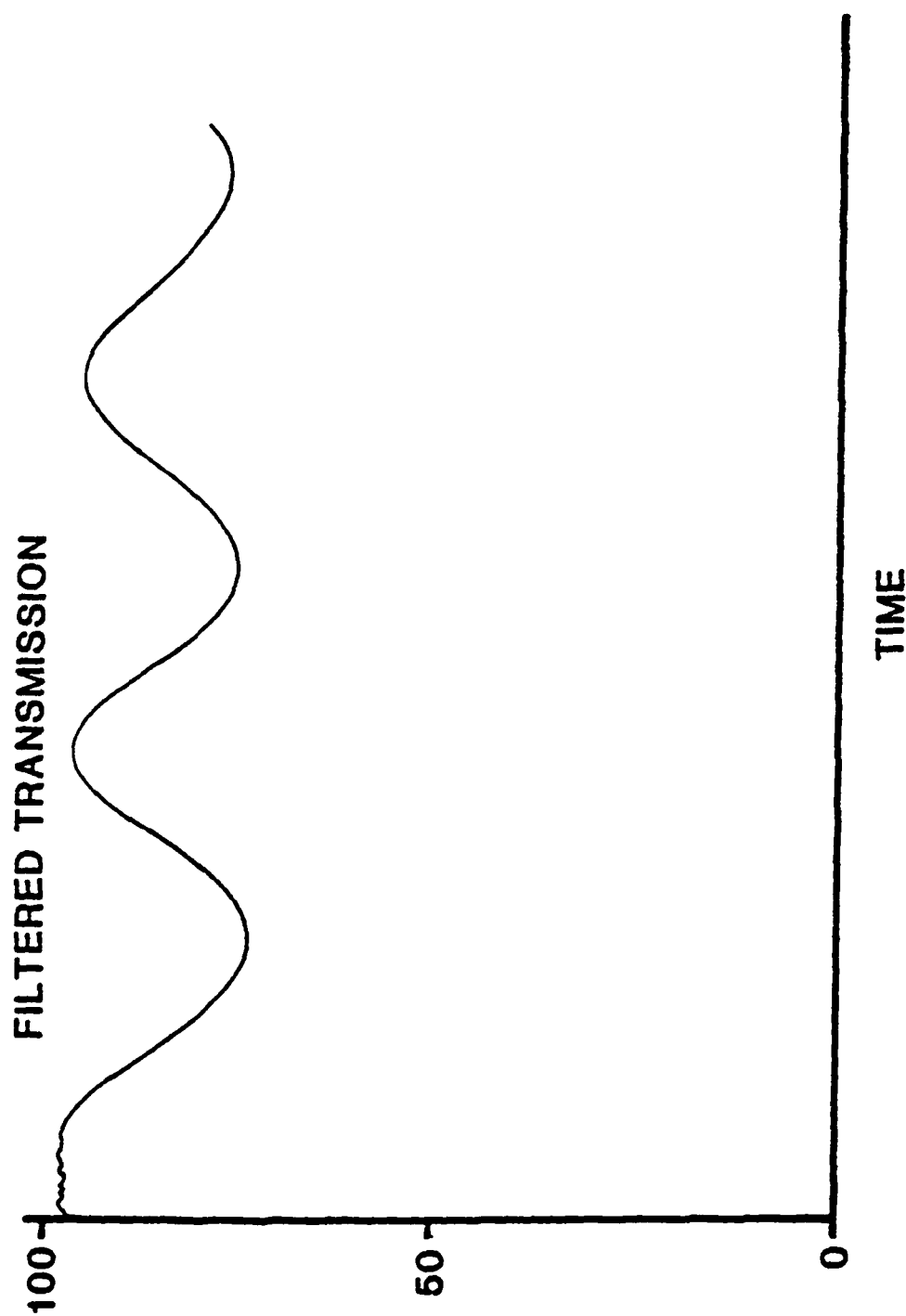


Fig 2. After filtering, the extrema have been extracted from the noise without distorting or attenuating the transmission curve.

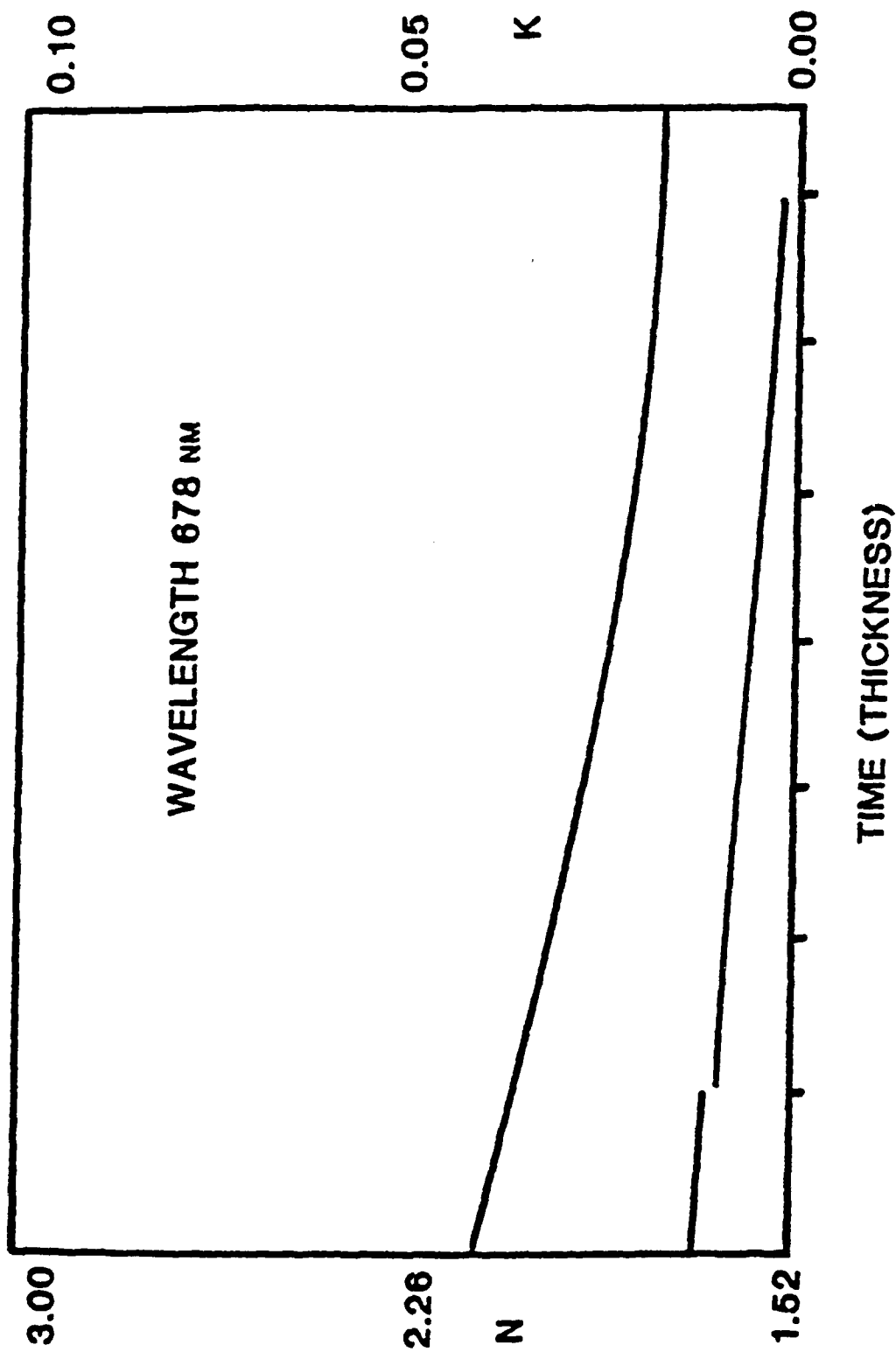


Fig 3. Profile of refractive index and extinction coefficient for a stable Titanium Dioxide layer. (Upper curve represents n, lower curve k).

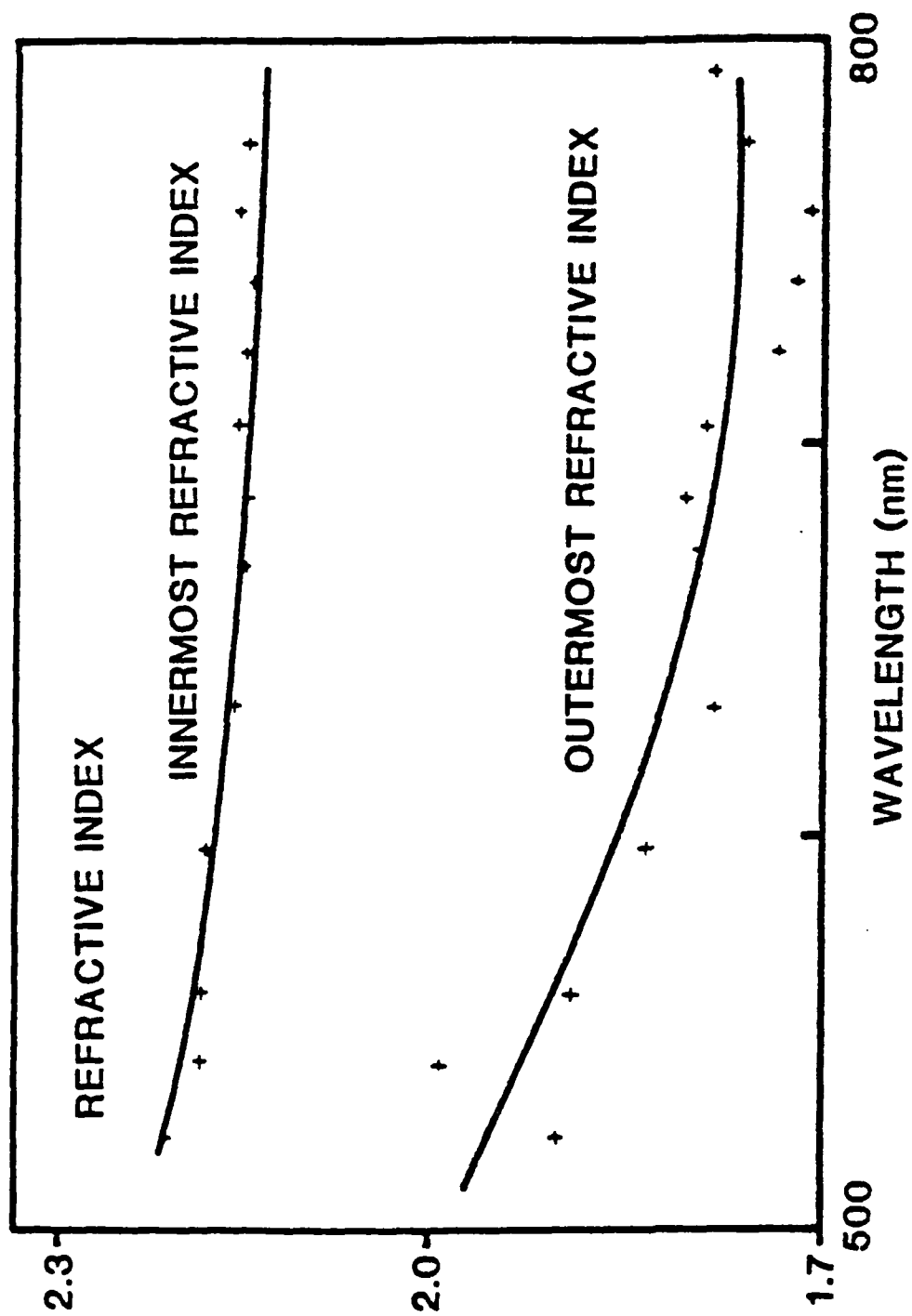


Fig 4. Dispersion of innermost and outermost refractive index for a stable layer of titanium dioxide.

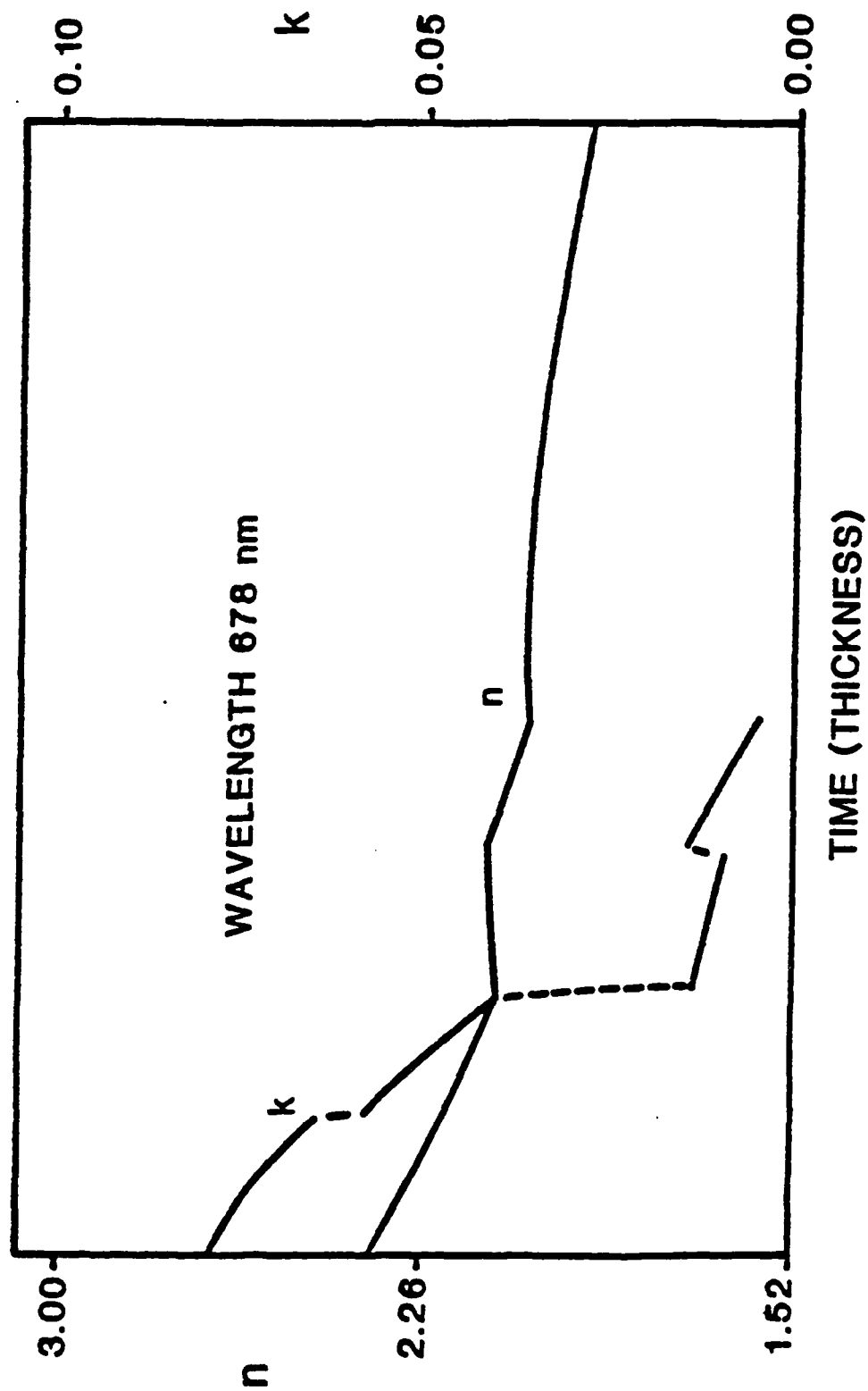


Fig 5. Example of result given by the method when applied to an unstable layer. Titanium dioxide layer deposited in an oxygen deficient atmosphere.

END

FILMED

4-85

DTIC